Aus der Klinik und Poliklinik für Nuklearmedizin
Klinik der Universität München
Direktor: Prof. Dr. Peter Bartenstein

Die Positronen-Emissions-Tomographie zur Beurteilung der zerebralen Amyloid-Verteilung sowie der pharmakologischen Effekte einer Serotonin-Wiederaufnahme-Hemmung

Dissertation
zum Erwerb des Doktorgrades der Medizin
an der Medizinischen Fakultät der
Ludwig-Maximilians-Universität zu München

vorgelegt von

Julia Johanna Sauerbeck

aus Burglengenfeld

2023

Mit Genehmigung der Medizinischen Fakultät der
Universität München

Berichterstatter:	Prof. Dr. Axel Rominger
Mitberichterstatter:	Prof. Dr. Michael Ewers
	PD Dr. Sven Lammich
Dekan:	Prof. Dr. med. Thomas Gudermann
Tag der mündlichen Prüfung:	25.05.2023

Die vorliegende kumulative Dissertation umfasst zwei bereits publizierte Manuskripte:

Sauerbeck J, Ishii K, Hosokawa C, Kaida H, Scheiwein FT, Hanaoka K, Rominger A, Brendel M, Bartenstein P, Murakami T.
The correlation between striatal and cortical binding ratio of 11C-PiB-PET in amyloid-uptake-positive patients
Ann Nucl Med. 2018 Jul;32(6):398-403. doi: 10.1007/s12149-018-1258-8. Epub 2018 May 5. PMID: 29730823.

Brendel M*, Sauerbeck J*, Greven S, Kotz S, Scheiwein F, Blautzik J, Delker A, Pogarell O, Ishii K, Bartenstein P, Rominger A; Alzheimer's Disease Neuroimaging Initiative.
Serotonin Selective Reuptake Inhibitor Treatment Improves Cognition and Grey Matter Atrophy but not Amyloid Burden During Two-Year Follow-Up in Mild Cognitive Impairment and Alzheimer's Disease Patients with Depressive Symptoms.
J Alzheimers Dis. 2018;65(3):793-806. doi: 10.3233/JAD-170387. PMID: 30010116.
*geteilte Erstautorenschaft

Kumulative Dissertation gemäß § 4a der Promotionsordnung

Inhaltsverzeichnis

1. Einführung

1.1. Demenz bei M. Alzheimer

Aufgrund der steigenden Alterung der Bevölkerung rücken Demenz-Erkrankungen zunehmend in den Fokus. Dem World Alzheimer Report 2018 zufolge soll die Zahl Demenzerkrankter von aktuell ca. 50 Millionen auf etwa 152 Millionen im Jahr 2050 ansteigen (Patterson 2018). Demzufolge belaufen sich die Kosten aktuell auf etwa eine Billion US-Dollar und sollen sich bis zum Jahr 2030 verdoppeln. Den größten Anteil, etwa zwei Drittel der Demenzerkrankungen, macht die Alzheimer-Demenz aus (Patterson 2018).

Die klinischen Diagnosekriterien der Demenz wurden 2011 vom National Institute on Aging-Alzheimer's Association erneuert: Eine Demenz zeichnet sich durch die progrediente Einschränkung der kognitiven Leistungsfähigkeit über einen Zeitraum von mindestens sechs Monaten aus, die mit einer Beeinträchtigung des alltäglichen Lebens einhergeht sowie nicht durch eine andere, zugrundeliegende Erkrankung erklärt werden kann. Bei der Alzheimer-Demenz im Speziellen zeigt sich ein langsam fortschreitender Progress, zunehmender Gedächtnisverlust oder Auffälligkeiten in Sprache und Exekutivfunktionen (McKhann, Knopman et al. 2011). Um die klinische Diagnose einer Alzheimer-Demenz stellen zu können, müssen die genannten klinischen Kriterien erfüllt sein. Ergänzend bzw. bei unklaren Fällen können Biomarker eingesetzt werden.

Die der Alzheimer-Demenz zugrundeliegende Pathologie ist vielfältig und bislang nicht abschließend geklärt. Einen wesentlichen Punkt stellt die Amyloid-Pathologie dar. Bereits Alois Alzheimer entdeckte die zerebralen Proteinablagerungen bei betroffenen Patienten, welche später als extrazelluläres β-Amyloid sowie intrazelluläres Tau bekannt wurden (Grontvedt, Schroder et al. 2018). Das Aβ-Peptid ist ein Spaltprodukt

aus dem Amyloid-Precursor-Protein (APP) und entsteht durch die Enzyme β- und γ-Sekretase. Es ist zwischen 36 und 43 Aminosäuren lang. Insbesondere Aβ-42 steht im Verdacht, amyloidogen zu wirken (Fukumoto, Asami-Odaka et al. 1996). Bei einem Ungleichgewicht zwischen Aβ-Auf- und Abbau kann es zur Bildung von Oligomeren und Fibrillen kommen. In akkumulierter Form entstehen fibrilläre Amyloid-Plaques, welche sich extrazellulär im Gehirn ablagern. Diese Amyloid-Ablagerungen entstehen Jahre bis Jahrzehnte vor der klinischen Erstmanifestation der Demenz-Erkrankung (Villemagne, Burnham et al. 2013). Das frühzeitige Auftreten dieser Ablagerungen stellt einen potenziellen therapeutischen Ansatzpunkt noch vor Beginn der ersten Symptome dar.

Zur Verlaufsbeurteilung der dementiellen Symptome wurden verschiedene Testverfahren entwickelt. Das im klinischen Alltag am häufigsten verwendete Testverfahren ist der Mini-Mental-Status-Test (MMSE, Mini Mental State Examination), der bei nur geringem Zeitaufwand eine erste Einschätzung des Demenzgrades erlaubt. Die Skala reicht von 0 bis 30 Punkten, wobei 30 Punkte das bestmögliche Ergebnis darstellen und von einer schweren Demenz bei unter 10 Punkten gesprochen wird (Creavin, Wisniewski et al. 2016). Eine weitere, häufig verwendete Testbatterie ist der Alzheimer's Disease Assessment Scale Cognition (ADAS-Cog), der etwas mehr Zeitaufwand benötigt und insbesondere eine gute Verlaufsbeurteilung ermöglicht. Bei diesem Test werden ausführlichere Aufgaben zu Gedächtnisleistung, Sprache und Orientierung gestellt. Die Skala beginnt bei 0 Punkten bei bestmöglichem Ergebnis, zeigt ab 10 Punkten eine kognitive Einschränkung an und reicht bis maximal 70 Punkten bei schwerster Demenz (Kueper, Speechley et al. 2018).

1.2. Diagnostik bei M. Alzheimer: Einsatz von Biomarkern und Positronen-Emissions-Tomographie (PET)

Bislang ist die Diagnosesicherung eines M. Alzheimer nur *post mortem* mit dem histologischen Nachweis von zerebralem Amyloid möglich, weshalb intensiv an der In-vivo-Diagnostik geforscht wird. Das langfristige Ziel besteht darin, frühe Stadien pathologischer Befunde erkennen und entsprechend noch vor bzw. bei Auftreten der ersten klinischen Symptome therapieren zu können. Hierbei kommt verschiedenen Biomarkern für zerebrale Amyloid-Ablagerungen wie z. B. der Bildgebung des zerebralen Amyloids mittels Positronenemissionstomographie (PET), auf welche im Folgenden genauer eingegangen wird, eine entscheidende Rolle zu (Jack and Holtzman 2013):

Für die PET wird durch eine radiochemische Synthese ein Trägermolekül mit Affinität zu einer spezifischen Zielstruktur, in diesem Fall Amyloid, an ein radioaktives Isotop gebunden. Dabei wird ein Isotop mit β+-Zerfall benötigt, z. B. Fluor-18 (^{18}F) oder Kohlenstoff-11 (^{11}C). Dieser radioaktive Tracer wird dem Patienten intravenös verabreicht und verteilt sich über den Blutpool im gesamten Körper. Der Tracer bindet schließlich an die Zielstruktur, z. B. Amyloid. Die radioaktive Substanz sendet Positronen aus, welche sich mit einem Elektron des umgebenden Gewebes auslöschen und dabei zwei Gammaquanten, hochenergetische Photonen, emittieren. Diese können durch die PET aufgezeichnet werden.

PET-Radiopharmaka, welche die β-Amyloid-Ablagerungen in-vivo sichtbar machen können, sind beispielsweise ^{18}F-Florbetaben (Barthel, Gertz et al. 2011, Chiaravalloti, Danieli et al. 2017), ^{18}F-Florbetapir (Joshi, Pontecorvo et al. 2012, Kobylecki, Langheinrich et al. 2015, Heurling, Leuzy et al. 2016, Jack, Bennett et al. 2018), ^{18}F-Flutemetamol (Curtis, Gamez et al. 2015, Leuzy, Savitcheva et al. 2019). Diese Tracer

werden zunehmend Bestandteil der klinischen Diagnostik (Johnson, Minoshima et al. 2013, Leuzy, Savitcheva et al. 2019, Trivino-Ibanez, Sanchez-Vano et al. 2019). Insbesondere in unklaren Fällen kann eine ergänzende Amyloid-PET-Bildgebung entscheidend bei der Diagnosestellung sein (Brendel, Schnabel et al. 2017, Schonecker, Prix et al. 2017).

Einer der ersten, seit Jahren etablierten Amyloid-Tracer ist ^{11}C-Pittsburgh Compound B (^{11}C-PiB) (Klunk, Engler et al. 2004, Rabinovici, Furst et al. 2007, Weiner, Aisen et al. 2010, Villemagne, Mulligan et al. 2012), welcher insbesondere stark an Aβ42-Fibrillen bindet (Yamin and Teplow 2017).

1.3. Methodische Analysen der Amyloid-PET-Bildgebung

Der erste verlässliche Amyloid-Ligand für das menschliche Gehirn ist Pittsburgh Compound B (PiB). Hierbei handelt es sich um ein Derivat von Thioflavin T. Das mit radioaktivem Kohlenstoff markierte ^{11}C-PiB besitzt eine hohe Affinität zu Aβ 40 und 42. Es konnte gezeigt werden, dass die in den PiB-Bilddaten dargestellten Verteilungsmuster gut mit den in post-mortem-Untersuchungen histologisch gesicherten Mustern korrelieren, wodurch sich ^{11}C-PiB zu einem verlässlichen Biomarker der Amyloidlast in vivo entwickelte (Ikonomovic, Klunk et al. 2008, Rowe, Ackerman et al. 2008). Eine erhöhte Amyloidlast zeigen insbesondere der präfrontale sowie temporoparietale Kortex, der posteriore zinguläre Kortex und Precuneus sowie das Striatum (Klunk, Engler et al. 2004, Buckner, Snyder et al. 2005, Engler, Forsberg et al. 2006).

Eine weitere entscheidende Entdeckung war, dass das Kleinhirn sowohl bei AD- als auch bei gesunden Patientengruppen keine erhöhte bzw. nur eine gering erhöhte Amyloidlast aufweist und keine signifikanten Unterschiede bezüglich der zerebellären

Amyloidlast zwischen AD- und gesunder Vergleichskohorte gefunden werden konnte (Rowe, Ackerman et al. 2008). Diese Information war wichtig für die Auswertung der PiB-Bilddaten, da das Zerebellum somit eine stabile Referenzregion darstellt.

1.4. Amyloid-Pathophysiologie und die Rolle des Striatums

Zur Abklärung der pathologischen Ablagerungen in Form von β-Amyloid wurde in Studien der longitudinale Verlauf der Ablagerungen sowie die spezifischen Ablagerungsmuster untersucht. Die hierfür durchgeführten Studien zeigten eine große Variabilität bezüglich ihrer Ergebnisse. Exemplarisch konnte in einer Studie gezeigt werden, dass der anteriore zinguläre Kortex (ACC) frühzeitig vermehrte Aβ-Ablagerungen aufweist (Sojkova, Zhou et al. 2011). Im Gegensatz dazu konnte eine andere Studie in dieser Region keine vermehrte Aβ-Akkumulation nachweisen (Villain, Chetelat et al. 2012). Eine weitere Studie, welche die Amyloid-Ablagerungen in Patienten mit MCI untersuchte, ergab eine signifikant erhöhte Akkumulation sowohl im anterioren und posterioren zingulären Kortex als auch im temporalen und parietalen Kortex sowie im Putamen (Koivunen, Scheinin et al. 2011). Villaein et al. konnten dagegen keine erhöhte Amyloid-Ablagerung putaminal nachweisen. Diese Studie zeigte wiederum eine erhöhte Akkumulationsrate im präfrontalen Kortex, der Insel sowie im Okzipitallappen (Villain, Chetelat et al. 2012). In einer Studie konnte gezeigt werden, dass das Amyloid-PET zur Baseline es ermöglicht, mit großer Genauigkeit regionale Muster in der Amyloid-PET im Verlauf bei Patienten mit einer Alzheimer-Demenz vorherzusagen (Guo, Brendel et al. 2017).

Auch die striatale Amyloidlast wurde untersucht, wobei eine starke Korrelation insbesondere zwischen ventralem Striatum und medialem Anteil der orbitofrontalen Region festgestellt werden konnte (Ishibashi, Ishiwata et al. 2014).

Die mangelnde Übereinstimmung in verschiedenen Studien bezüglich der zerebralen Regionen mit erhöhter Amyloid-Akkumulationsrate kann möglicherweise auf unterschiedliche Krankheitsstadien der Patienten, unterschiedliche Länge der Studiendauer sowie die Wahl der Referenzregion zurückzuführen sein. Es wird angenommen, dass das Verteilungsmuster im Krankheitsverlauf nicht konstant ist, sondern einige Regionen frühzeitig einen erhöhten Amyloid-Tracer-Uptake zeigen, während andere in einem späteren Stadium eine erhöhte Amyloidlast aufweisen. Bei der Einteilung der Amyloidlast haben sich die Braak-Stadien etabliert (Braak and Braak 1995). Diese beschreiben das zerebrale Ausbreitungsmuster der Neurofibrillären Bündel im zeitlichen Verlauf. Dabei werden 5 Stadien beschrieben: Im Stadium I und II ist hauptsächlich der transentorhinale Kortex betroffen. Im Stadium III und IV zeigt sich zudem eine Ausdehnung in limbische Regionen wie den Hippocampus. Zuletzt, in den Stadien V und VI, ist der gesamte Neokortex betroffen.

Die dynamische Entwicklung der zerebralen Amyloidlast erfordert daher auch zukünftig ergänzende Studien.

Im ersten Teil der vorliegenden Promotionsarbeit wurden PiB-positive Patienten mit neurodegenerativer Grunderkrankung hinsichtlich der striatalen Amyloidlast und möglichen Verbindungen zu kortikalen Arealen ausgewertet.

1.5. Therapeutische Möglichkeiten

Aktuell stehen nur begrenzte, den Krankheitsverlauf verzögernde Therapiemöglichkeiten der Alzheimer-Demenz zur Verfügung. Eine kurative Therapieoption ist bislang nicht bekannt. Deshalb wurde und wird ausgiebig an therapeutischen Möglichkeiten geforscht.

Die aktuell zugelassenen Therapeutika sollen die kognitiven und motorischen Symptome lindern und den Krankheitsprogress verzögern. Cholinesterase-Inhibitoren wie Donepezil oder Rivastigmin sowie NMDA-Antagonisten wie Memantin können den Krankheitsstatus stabilisieren sowie eine Verschlechterung hinauszögern (Tan, Yu et al. 2014). Cholinesterase-Hemmer werden dabei bevorzugt bei beginnender dementieller Symptomatik bis MCI verwendet, NMDA-Antagonisten sind das Therapeutikum der Wahl bei moderater bis starker Ausprägung der Alzheimer-Erkrankung (Epperly, Dunay et al. 2017).

Zudem werden neuere Therapien entwickelt, welche versuchen an den Amyloidablagerungen anzugreifen. Dafür ist es einerseits notwendig, initiale Amyloidablagerungen nachzuweisen sowie andererseits deren Entwicklung im Verlauf verfolgen zu können (Nordberg, Rinne et al. 2010), weshalb die molekulare Bildgebung zunehmend nicht nur in der Diagnostik, sondern auch in der Therapie neurodegenerativer Erkrankungen eine wichtige Rolle spielt. Doch obwohl zahlreiche Studien zur Entwicklung anti-amyloidogener Therapien initiiert wurden und werden, scheitert der überwiegende Teil bislang aufgrund fehlender bzw. nur geringer Verbesserung des Outcomes (Kozin, Barykin et al. 2018, van Dyck 2018). 2021 wurde der erste monoklonale Antikörper gegen β-Amyloid, Aducanumab, durch die FDA zugelassen (Mukhopadhyay and Banerjee 2021). Es konnte gezeigt werden, dass durch Aducanumab die Bildung zerebraler Amyloid-Plaques reduziert werden kann (Sevigny, Chiao et al. 2016, Budd Haeberlein, Aisen et al. 2022). Da das Überwiegen des klinischen Nutzens gegenüber den Nebenwirkungen jedoch nicht eindeutig belegt werden konnte, wurde eine Zulassung durch die EMA bislang abgelehnt. Dies soll in aktuell laufenden Studien weiter analysiert werden.

In retrospektiven Analysen wurde gezeigt, dass bei klinischen Studien z. T. in mehr als einem Drittel der behandelten Patienten die therapeutische Zielstruktur, z. B. Amyloid-Plaques, nicht nachgewiesen werden konnte (Sevigny, Suhy et al. 2016). In diesen Fällen kann dadurch ein fehlendes/ unzureichendes Therapieansprechen erklärt werden (Vellas, Carrillo et al. 2013). Molekulare Biomarker werden daher zunehmend ein notwendiges Einschlusskriterium für aktuelle Studien bezüglich der Alzheimer-Erkrankung (Wolz, Schwarz et al. 2016).

Einen weiteren therapeutischen Ansatzpunkt stellen Selektive Serotonin-Reuptake-Inhibitoren (SSRI) dar. Es wird angenommen, dass Serotonin die Aβ-Produktion reduzieren kann (Reynolds, Mason et al. 1995). In früheren Studien konnte gezeigt werden, dass klinisch unauffällige Patienten mit SSRI-Einnahme in der Vergangenheit in der ^{11}C-PiB-PET eine signifikant geringere Amyloidlast aufwiesen im Vergleich zur Kontrollgruppe ohne SSRI-Einnahme (Cirrito, Disabato et al. 2011). Darüber hinaus konnte in der gleichen Studie eine negative Korrelation zwischen Amyloidlast und Dauer der SSRI-Einnahme gezeigt werden.

In einer präklinischen Studie mit prospektivem Studiendesign konnte ein Stillstand des Wachstums vorbestehender Amyloid-Plaques sowie eine Hemmung neuer Plaques um 78% in transgenen AD-Mäusen nachgewiesen werden (Sheline, West et al. 2014).

Bislang ist die Auswirkung einer SSRI-Einnahme beim Menschen in Zusammenhang mit der Alzheimer-Erkrankung nicht ausreichend geklärt und weiterhin Gegenstand der Forschung, weshalb sich der zweite Teil dieser Promotionsarbeit diesem Thema gewidmet hat.

1.6. Alzheimer's Disease Neuroimaging Initiative (ADNI)

Bei der Alzheimer's Disease Neuroimaging Initiative (ADNI) handelt es sich um ein multizentrisches Forschungsprojekt, welches sich zum Ziel gesetzt hat, die Prävention, Diagnostik und Behandlung der Alzheimer-Erkrankung zu verbessern.

Das Projekt wurde 2004 ins Leben gerufen. Seitdem werden dafür an 57 Zentren in den Vereinigten Staaten sowie Kanada Daten erhoben. Hierbei handelt es sich um Bilddaten von PET- sowie MRT-Untersuchungen, klinische, kognitive, genetische und biochemische Biomarker von gesunden Patienten, Patienten mit leichter kognitiver Einschränkung bis hin zu Patienten mit vollständiger klinischer Ausprägung einer Alzheimer-Demenz. Die Daten werden zur Baseline sowie in regelmäßigen Abständen im Verlauf erhoben, um eine longitudinale Beobachtung zu ermöglichen. Diese umfangreiche Datenbank wird Wissenschaftlern weltweit zugänglich gemacht, um die Erforschung der Pathophysiologie, Diagnostik und Therapie der Alzheimer-Erkrankung voranzutreiben (Weiner, Aisen et al. 2010, Weiner, Veitch et al. 2017). Die Daten-Grundlage der zweiten Publikation der vorliegenden Dissertation stellt diese Datenbank dar. Im Rahmen der geteilten Erstautorenschaft wurde gemeinschaftlich mit Herrn PD Dr. Brendel das Studiendesign erarbeitet. Nachdem ich die statistische Auswertung durchführte, erfolgten in enger Zusammenarbeit die Diskussion und Interpretation der Ergebnisse und gemeinsame Verfassung des vorliegenden Papers.

2. Inhalte der Promotionsarbeit

2.1. Die Korrelation zwischen striataler und kortikaler Amyloidlast in in Amyloid-positiven Patienten

Im Rahmen der ersten Arbeit der vorliegenden Dissertation wurde das Ausbreitungsmuster der zerebralen Amyloidlast mittels ^{11}C-PiB-PET-Bildgebung untersucht. Das Hauptaugenmerk lag hierbei auf der Korrelation zwischen striataler und kortikaler Amyloidablagerung in Amyloid-positiven Patienten.

Hierfür wurden 73 Amyloid-positive Patienten eingeschlossen (31 männlich/ 42 weiblich) mit einem mittleren Alter von 71,5 ± 2,1 Jahren und einem mittleren MMSE-Wert von 21,7 ± 1,4. Dieses Patientenkollektiv wurde sowohl mittels FDG-PET des Gehirns als auch mit ^{11}C-PiB-PET (dynamisch) untersucht. Unter den 73 ausgewählten Patienten befanden sich 34 mit AD, 26 mit MCI, 2 mit frontotemporaler Lobärdegeneration (FTLD), 2 mit einer Parkinson-Erkrankung, 5 mit einer Lewy-Körperchen-Erkrankung und 4 mit dementieller Symptomatik ohne klare Diagnose. Zur Diagnosestellung wurden die Kriterien der „Neurological and Communicative Disorders and Stroke-Alzheimer's Diesease and Related Disorders Association for AD" und die dritte Ausgabe des „Dementia with Lewy Bodies Consortium" angewendet.

Die FDG-PET-Scans wurden bei nüchternen Patienten 30 Minuten nach der intravenösen Injektion über 30 Minuten in einem statischen Fenster akquiriert. Die ^{11}C-PiB-PET-Scans dagegen wurden dynamisch über 70 Minuten ab i.v.-Injektionszeitpunkt akquiriert. Anschließend wurden die Bindungspotentiale mittels PMOD analysiert. Parametrische Bilder der regionalen ^{11}C-PiB-Aufnahme wurden mittels Logan Graphical Analysis mit dem Zerebellum als Referenzregion generiert.

Für die Aufnahmen zur Analyse der Bindungspotentiale wurden alle dynamischen Daten ab Injektionszeitpunkt bis 70 Minuten p.i. genutzt und anschließend auf die

individuellen FDG-Bilder coregistriert, räumlich normalisiert (auf den Montreal Neuorologic Institute (MNI) Standard Space) und mit einem Gauss-Filter von 8 mm geglättet. Die individuellen Werte der Bindungspotentiale wurden mithilfe des Zerebellums normalisiert. Es wurden statistische parametrische Vergleiche mittels SPM8 durchgeführt, um Korrelationen zwischen striataler und kortikaler Bindungspotential-Werte erstellen zu können. Dies beinhaltete eine multiple Regression, um sowohl positive als auch negative Korrelationen erkennen zu können. Ein p-Wert von weniger als 0,05 Familywise Error (FWE) für multiple Vergleiche wurde dabei als statistisch signifikant gewertet. Hierbei wurden multiple positive Korrelationen, jedoch keine negativen entdeckt. Es zeigte sich beim Vergleich der striatalen zu den kortikalen BP_{ND}-Werten eine signifikante Korrelation zwischen Striatum und präfrontalem Kortex. Die stärkste Korrelation wies dabei das Brodmann-Areal 11 der linken Seite auf. Das Brodmann Areal 11 ist eine wichtige Struktur für Lern-Prozesse, insbesondere das Extinktionslernen, sowie für die Entscheidungsfindung. Am Entscheidungsprozess ist auch das Striatum beteiligt. Die signifikanten Korrelationen sind im Detail in der Tabelle 1 aufgelistet.

Brodmann-Areal	Gehirn-Region	Seite	Koordinaten			T-Werte
			X	Y	Z	
BA 11	Orbitofrontaler Kortex	links	-9	33	-9	17,49
BA11	Orbitofrontaler Kortex	rechts	1	26	-12	16,80
BA 32	Dorsaler anteriorer zingulärer Kortex	links	-8	35	11	15,46
BA 32	Dorsaler anteriorer zingulärer Kortex	rechts	11	37	7	15,24
BA 45	Broca-Areal	rechts	32	25	6	14,43
BA 9	Dorsolateraler/ medialer präfrontaler Kortex	links	-37	21	25	14,26
BA 9	Dorsolateraler/ medialer präfrontaler Kortex	rechts	37	28	24	14,15
BA 46	Dorsolateraler präfrontaler Kortex	rechts	37	39	13	14,10
BA 31	Dorsaler posteriorer zingulärer Kortex	links	-11	-55	29	14,09
BA 10	Präfrontaler Kortex	links	-33	43	3	13,88
BA 10	Präfrontaler Kortex	rechts	7	46	-11	13,46

Tabelle 1. Signifikante Korrelation zwischen kortikalem und striatalem Bindungspotential.

Abbildung 1 zeigt die Korrelationen anhand einer Oberflächenprojektion. Hier zeigen sich ausgedehnte Areale mit signifikanter Korrelation. Eine Ausnahme bilden dabei die zerebellären Hemisphären. Die stärkste Korrelation zeigt sich frontobasal, die schwächste Korrelation in okzipitalen Arealen. Zusammenfassend zeigten sich multiple, positive Korrelationen zwischen striataler und kortikaler Amyloidablagerung. Von diesen kortikalen Arealen sind sowohl funktionelle als auch anatomische Verbindungen zum Striatum bekannt. Deshalb scheint es wahrscheinlich, dass die Ausbreitung der Amyloidplaques nicht zufällig stattfindet, sondern von funktionellen und anatomischen Verbindungen abhängig ist.

Diese Ergebnisse wurden 2018 im Rahmen der ersten Erstautorenschaft „The correlation between striatal and cortical binding ratio of ^{11}C-PiB PET in amyloid-uptake-positive patients“ in Annals of Nuclear medicine veröffentlicht (Sauerbeck, Ishii et al. 2018).

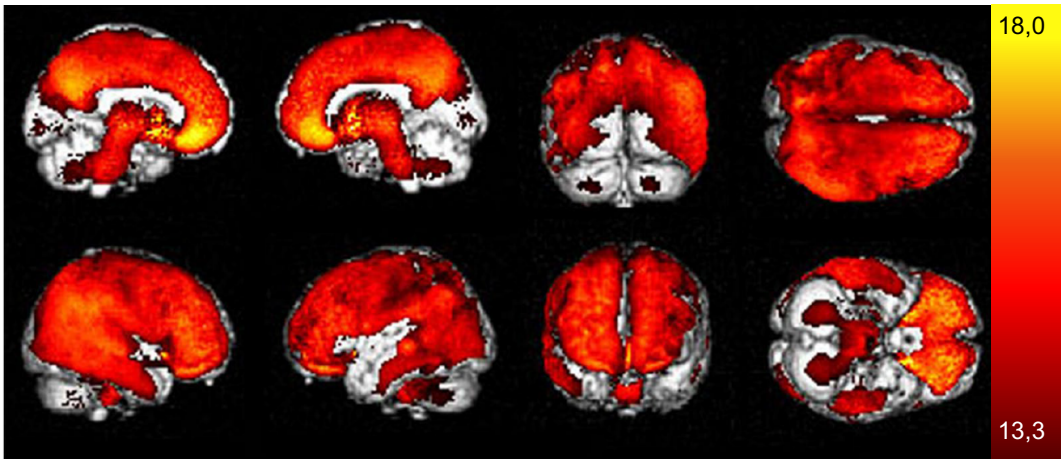

Abbildung 1. Signifikante Korrelationen zwischen kortikaler und striataler Amyloidlast. Die deutlichste Assoziation ist frontobasal zu beobachten (gelb).

2.2. Selektive Serotonin-Wiederaufnahmehmmer (SSRI) verbessern Kognition und Atrophie der grauen Substanz, jedoch nicht die Amyloidlast im 2-Jahres-Verlauf in Patienten mit leichter kognitiver Einschränkung (MCI) und M. Alzheimer mit depressiver Symptomatik

Im Rahmen der zweiten Publikation wurde der Einfluss selektiver Serotonin-Wiederaufnahme-Hemmer (SSRI) auf Kognition, zerebrale Atrophie und Amyloidlast untersucht. Für diese Fragestellung wurde ein Kollektiv der ADNI-Datenbank genutzt. Zum Einschlussdatum waren 409 passende Patienten verfügbar, welche entweder einer gesunden Kontrollgruppe angehörten oder die Diagnose einer MCI/ AD erhalten hatten. Zudem hatten alle eingeschlossenen Patienten ein Amyloid-PET mit ^{18}F-AV45 (Florbetapir) sowie ein MRT sowohl zur Baseline als auch im Zwei-Jahres-Follow-Up erhalten.

Anhand der Mini Mental State Examination (MMSE) sowie mithilfe klinischer Kriterien, gemessen am Clinical Dementia Rating (CDR), wurden die Probanden in HC, MCI und AD unterteilt. Zusätzlich wurde der Apolipoprotein-E4-Status (ApoE4), das Geschlecht sowie die Bildungsjahre erhoben. Zum Zeitpunkt der Bildakquise erfolgte zudem die Aufzeichnung des Alters, NPI-Q-Scores und des ADAS-Scores. Die Patienten konnten somit unterteilt werden in eine gesunde Vergleichskohorte (N = 153) und Patienten mit MCI oder AD (N = 256).

Mit Hilfe des Neuropsychiatric Inventory–Questionnaire-Scores (NPI-Q-Scores) (Item 4; Depressive Symptome) wurden die Gruppen weiter unterteilt in Probanden mit respektive ohne depressive Symptomatik zum Zeitpunkt des Baseline-Scans. Die Patienten mit depressiver Symptomatik wurden weiter unterteilt in eine Gruppe mit und eine Gruppe ohne SSRI-Therapie unterteilt.

Die MCI-/ AD-Gruppe wurde dementsprechend aufgeschlüsselt in drei Untergruppen:

a) Patienten mit depressiver Symptomatik und SSRI-Behandlung (N = 24)
b) Patienten mit depressiver Symptomatik, jedoch ohne SSRI-Behandlung (N = 49)
c) Patienten ohne depressive Symptomatik (N = 183).

Die Patienten mit demenzieller Symptomatik wurden zudem unterteilt in eine Amyloid-positive und eine Amyloid-negative Untergruppe entsprechend der Amyloidlast im PET-Befund zur Baseline. Für diese Einteilung wurde zunächst ein Zielvolumen (Volume of Interest; VOI) für die Auswertung der Amyloid-PET gebildet, welches die Summe der Amyloidlast aus frontaler, temporaler, parietaler grauer Substanz sowie des posterioren Gyrus cinugli/ Precuneus darstellt. Dieser Wert wurde anschließend durch die Amyloidlast einer Referenz-Region geteilt. Als Referenzregion wurde die weiße Substanz gewählt, da diese die genaueste Unterscheidung zwischen HC und AD ermöglicht (Brendel, Hogenauer et al. 2015). Dadurch ergibt sich das Verhältnis des standardisierten Aufnahmewertes des Tracers (als Korrelat zur Amyloidlast) zur Referenz-Region (Standardized Uptake Value Ratio, SUVR). Die statistischen Analysen erfolgten in SPSS mittels einer multivariaten Kovarianzanalyse und wurden Bonferroni-adjustiert. Das Ziel meiner Promotionsarbeit war, die Effekte einer Therapie

mit SSRI auf Alzheimer-Patienten (AD) sowie Patienten mit einer leichten, kognitiven Einschränkung (MCI) zu untersuchen.

In Bezug auf die kognitive Leistungsfähigkeit konnte in der longitudinalen Analyse kein Unterschied zwischen Patienten mit bzw. ohne depressive Symptomatik beobachtet werden. Jedoch konnte eine signifikante Verbesserung der Kognition innerhalb der Gruppe der Patienten mit depressiver Symptomatik und SSRI-Behandlung, gemessen an einer Abnahme des ADAS, gezeigt werden (absolut: -0,8 / relativ: –5,0%). Im Gegensatz dazu zeigte sich bei der Gruppe ohne SSRI-Behandlung eine Verschlechterung der Kognition und dementsprechend ein Anstieg des ADAS (absolut: +2,9 / relativ: +18,6%; p = 0,013, Abbildung 2). In der Untergruppe der Amyloid-positiven Patienten mit depressiver Symptomatik konnte der gleiche, wenn auch nicht signifikante Trend, nachgewiesen werden.

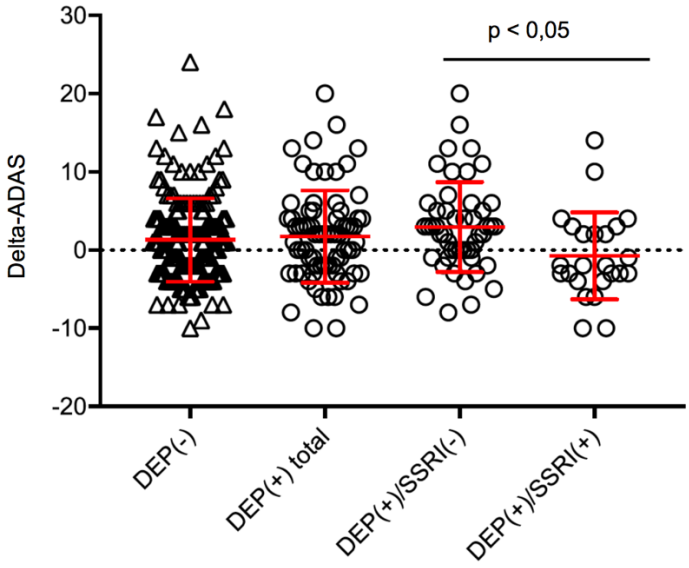

Abbildung 2. Entwicklung des ADAS im 2-Jahres-Verlauf für Patienten mit respektive ohne depressive Symptomatik sowie die Untergruppen der Patienten mit bzw. ohne SSRI-Medikation.

Des Weiteren wurde untersucht, wie sich die Demenz-Diagnosen im Verlauf von Baseline zu Follow-Up veränderten. 29 der 225 Patienten, die zur Baseline als MCI eingestuft wurden, zeigten eine Konversion zur Demenz vom Alzheimer-Typ. 10 der

225 Patienten dagegen verbesserten sich, sodass sie zum Follow-Up als HC gewertet wurden.

Von insgesamt 31 AD-Patienten zur Baseline zeigte ein Fall eine Konversion zu MCI, der Großteil (96,8%) wies unverändert die Diagnose AD auf.

Basierend auf präklinischen Ergebnissen (Cirrito, Disabato et al. 2011) war ein wesentlicher Bestandteil der Analyse die longitudinale Untersuchung der Amyloidlast. Es zeigten sich insgesamt Tendenzen, jedoch keine signifikanten Unterschiede im 2-Jahres-Verlauf: Zwischen subsyndromal depressiven und nicht-depressiven Patienten konnte im Gesamthirn kein wesentlicher Unterschied im Anstieg der Amyloidlast im 2-Jahres-Verlauf (∆%-SUVR: +5,0% versus +5,6%; p = 0,568) nachgewiesen werden. In der Untergruppe der subsyndromal depressiven Patienten mit SSRI-Therapie zeigte sich ein tendentiell geringerer, jedoch nicht-signifikanter Anstieg des zerebralen Amyloids mit stärkster Ausprägung im frontalen Kortex im Vergleich zu den subsyndromal depressiven Patienten ohne SSRI-Therapie (∆%-SUVR: +5,0% versus +6,1%; p = 0,635). Die ergänzende Analyse ausschließlich der Amyloid-positiven Patienten führte zu einem ähnlichen Ergebnis.

In einem weiteren Schritt wurde die zerebrale Atrophierate anhand des MRTs untersucht: Im Vergleich der subsyndromal depressiven und der nicht-depressiven Patientengruppe zeigte sich kein signifikanter Unterschied bezüglich des Rückgangs des gesamten Volumens der grauen Substanz sowie der Volumina der Einzelregionen im beobachteten Zeitraum.

In der Analyse der Untergruppen konnte gezeigt werden, dass Patienten mit subsyndromaler Depression ohne SSRI-Behandlung einen Rückgang von 2,7% des Gesamtvolumens aufwiesen, wohingegen subsyndromal depressive Patienten unter

SSRI-Behandlung einen signifikant geringeren Rückgang von 0,9% zeigten (p = 0,031). Die höhere Atrophierate der grauen Substanz in der Gruppe der subsnydromal depressiven Patienten ohne SSRI-Behandlung konnte betont im frontalen (Volumenveränderung frontal: –0,8% versus -2,7%; p = 0,042) sowie temporalen Kortex gezeigt werden (Volumenveränderung temporal: -0,9% versus -2,6%; p = 0,016).

Unter den Amyloid-positiven Patienten konnte eine signifikant höhere durchschnittliche zerebrale Atrophierate bei subsyndromaler Depression gezeigt werden verglichen mit der Gruppe ohne depressive Symptomatik. Beispielsweise wiesen das Gesamtvolumen der grauen Substanz (Volumenänderung –1,4% versus –3,8%; p = 0,040) und der temporale Kortex (Volumenänderung –1,1% versus –3,9%; p = 0,009) in dieser Gruppe eine signifikant geringere Abnahme auf als in der Vergleichsgruppe ohne SSRI-Behandlung. Zur Veranschaulichung werden in Tabelle 2 zwei exemplarische Fälle gezeigt.

Gruppe	ADAS		Baseline Amyloid-PET	cMRT	
	Baseline	Follow-Up		Baseline	Follow-Up
Pat. mit depressiver Symptomatik ohne SSRI-Therapie	23	43	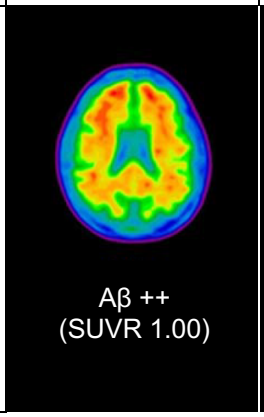 Aβ ++ (SUVR 1.00)	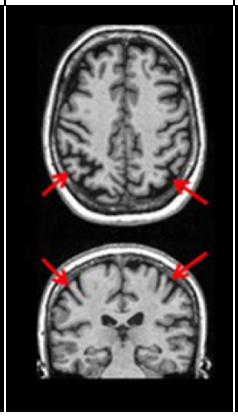	

Pat. mit depressiver Symptomatik und SSRI-Therapie	29	26	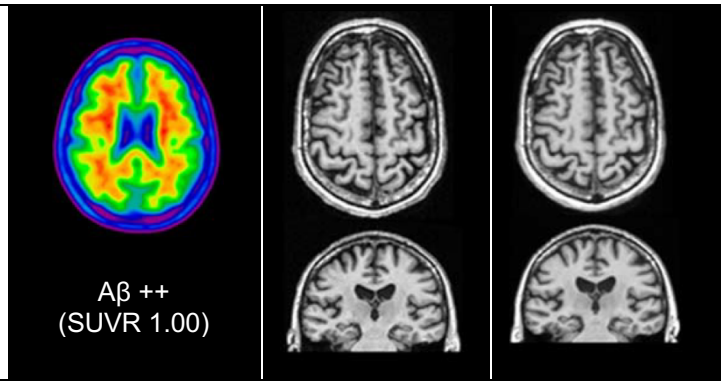

Tabelle 2. Zwei zur Baseline vergleichbare, Amyloid-positive Patienten mit depressiver Symptomatik. Es zeigt sich eine visuell deutlichere Atrophie im 2-Jahres-Verlauf in dem Patienten ohne SSRI-Therapie im Vergleich zu dem Patienten unter SSRI-Therapie.

Zusätzlich zu o. g. Analysen wurde die Amyloidlast zur Baseline korreliert mit dem longitudinalen, klinischen Verlauf. Wir führten hierzu Regressionsanalysen durch: Die Amyloidlast zum Zeitpunkt der Baseline korrelierte positiv mit dem longitudinalen, kognitiven Verlauf. Derselbe Trend zeigte sich bei der Untergruppe der subsyndromal depressiven Patienten unter SSRI-Behandlung, hier konnte jedoch keine Signifikanz erreicht werden.

Die Ergebnisse weisen darauf hin, dass Patienten mit MCI oder AD bezüglich der kognitiven Leistungsfähigkeit von einer Behandlung mit SSRI profitieren. Das morphologische Korrelat hierzu waren geringere Atrophieraten der grauen Substanz bei Patienten unter SSRI-Therapie. Jedoch wurden nur 33% der Patienten mit depressiver Symptomatik mit SSRI behandelt. Aufgrund des geringen Anteils mit SSRI behandelter Patienten bei subsyndromaler Depression legen unsere Ergebnisse nahe, das Augenmerk zunehmend auf die ausreichende, medikamentöse Behandlung einer depressiven Symptomatik zu legen. Dies könnte, auch wenn keine manifeste Depression vorliegt, das kognitive Outcome verbessern. Im Gegensatz zum Tiermodell konnten in unserer Analyse jedoch keine signifikanten Einflüsse der SSRI-Therapie auf die Veränderung der Amyloidlast nachgewiesen werden. Hier können prospektive Studien mit einheitlichem Beginn einer SSRI-Medikation in einem frühen Krankheitsstadium und Beobachtung über einen längeren Verlauf hilfreich sein.

Die Ergebnisse wurden 2018 im Rahmen der geteilten Erstautorenschaft „Serotonin Selective Reuptake Inhibitor Treatment Improves Cognition and Grey Matter Atrophy but not Amyloid Burden During Two-Year Follow-Up in Mild Cognitive Impairment and Alzheimer's Disease Patients with Depressive Symptoms" veröffentlicht (Brendel, Sauerbeck et al. 2018).

3. Zusammenfassung

In dieser Promotionsarbeit wurde mithilfe der Positronen-Emissions-Tomographie (PET) die zerebrale Amyloid-Verteilung im Hinblick auf das Verteilungsmuster sowie im longitudinalen Verlauf, insbesondere bei Patienten mit subsyndromaler Depression und SSRI-Einnahme, untersucht.

Im ersten Teil der vorliegenden Promotionsarbeit wurde der Zusammenhang zwischen striataler und kortikaler Amyloidlast untersucht, um das Ausbreitungsmuster der zerebralen Amyloidlast und somit die regionalen zerebralen Verbindungen besser verstehen zu können. Dafür untersuchten wir 73 Amyloid-positive Patienten mit einer neurodegenerativen Erkrankung mit einem durchschnittlichen Alter von 71,5 ± 1,4 Jahren. Die neurodegenerativen Erkrankungen beinhalteten die Alzheimer-Demenz (AD, N = 34), leichte kognitive Einschränkungen (MCI) aufgrund einer Alzheimer-Demenz (N = 26), frontotemporale Lobärdegeneration (N = 2), M. Parkinson (N = 2), Lewy-Körperchen-Demenz (N = 5) sowie Patienten mit dementieller Symptomatik unklarer Genese (N = 4). Alle Patienten erhielten sowohl eine Glukose-PET- als auch eine Amyloid-PET-Untersuchung mit ^{11}C-PiB des Gehirns.

Für die ^{11}C-PiB-PET-Scans wurde eine durchschnittliche Dosis von 555 ± 185 MBq ^{11}C-PiB intravenös appliziert und die Bilder dynamisch über 70 Minuten ab dem Applikationszeitpunkt akquiriert. Zur Analyse wurden die PiB-PET-Bilder co-registriert auf die individuellen FDG-PET-Bilder und anschließend räumlich normalisiert. Weiterhin wurden die Bilder geglättet und auf das Zerebellum normalisiert. Darauf basierend wurde eine voxelweise Analyse mittels SPM8 durchgeführt, wobei mittels multipler Regression sowohl mögliche positive als auch negative Korrelationen ermittelt werden konnten.

Die Ergebnisse ergaben signifikante, ausschließlich positive Korrelationen zwischen striataler und kortikaler Amyloidlast, wobei sich die stärkste Korrelation frontobasal im linken Brodmann-Areal 11 abgrenzen ließ. Zerebellär konnte dagegen keine signifikante Korrelation gefunden werden.

Zwischen den striatalen und kortikalen Arealen mit signifikanter Korrelation sind anatomische sowie funktionelle Verbindungen bekannt. Dies legt die These nahe, dass die Amyloid-Verteilung im Gehirn funktionellen und anatomischen Verknüpfungen folgt. Zukünftige, longitudinale Studien können helfen, die Verteilungsmuster im longitudinalen Verlauf besser zu verstehen.

Der zweite Teil der vorliegenden Promotionsarbeit beschäftigt sich mit dem Einfluss selektiver Serotonin-Reuptake-Inhibitoren (SSRI) auf die kognitive Leistungsfähigkeit, Atrophie der grauen Substanz und Amyloidlast bei Patienten mit einer Demenz vom Alzheimer Typ oder mit einer leichten kognitiven Störung im 2-Jahres-Verlauf.

Präklinische Studien legten im Maus-Modell nahe, dass die Gabe von SSRI die Amyloidogenese verzögern kann. Basierend auf dieser These untersuchten wir retrospektiv den Einfluss einer SSRI-Therapie auf die zerebrale Amyloidlast, kognitive Leistungsfähigkeit und Atrophie der grauen Substanz in subsyndromal depressiven Patienten mit MCI oder AD im 2-Jahres-Verlauf. Es wurden 256 Patienten aus der ADNI-Datenbank untersucht, hiervon 225 mit MCI und 31 mit einer Demenz vom Alzheimer-Typ. Diese Patienten hatten sowohl ein Amyloid-PET als auch ein MRT zur Baseline und im 2-Jahres-Follow-Up. Des Weiteren wurden die Patienten mit depressiver Symptomatik unterteilt in Patienten mit (N = 24) respektive ohne (N = 49) SSRI-Medikation.

Die Entwicklung der kognitiven Leistungsfähigkeit wurde mithilfe der Differenz des ADAS vom Baseline- zum Follow-Up-Zeitpunkt dargestellt. Die Amyloid-Ablagerung wurde durch das Amyloid-PET quantifiziert mit der weißen Substanz als Referenzregion. Die Analysen wurden jeweils unter Einbezug der Kovariablen Alter, Geschlecht, Bildungsjahre, ApoE4-Status durchgeführt. Ergänzend wurden die Analysen auch in der Subgruppe der Amyloid-positiven Patienten durchgeführt.

Patienten mit depressiver Symptomatik unter SSRI-Behandlung zeigten einen signifikant geringeren Abfall der kognitiven Leistungsfähigkeit im 2-Jahres-Verlauf im Vergleich zu Patienten mit depressiver Symptomatik, die keine SSRI-Behandlung erhalten haben. Dabei konnte kein Zusammenhang mit der Amyloidlast zur Baseline nachgewiesen werden. Im 2-Jahres-Verlauf konnten nur angedeutete, nicht signifikante Trends eines positiven Einflusses der SSRI-Medikation auf die Amyloidlast gezeigt werden.

Die vorliegenden Ergebnisse weisen darauf hin, dass Patienten mit einer leichten kognitiven Störung oder einer Alzheimer-Demenz bezüglich der kognitiven Leistungsfähigkeit von einer Therapie mit SSRI profitieren. Das morphologische Korrelat hierzu waren geringere Atrophieraten der grauen Substanz in Patienten mit SSRI-Behandlung. Aufgrund der verhältnismäßig geringen Anzahl mit SSRI therapierter Patienten bei subsyndromaler Depression legen unsere Ergebnisse nahe, das Augenmerk zunehmend auf die ausreichende, medikamentöse Behandlung einer depressiven Symptomatik zu legen, auch wenn keine manifeste Depression vorliegt, um das kognitive Outcome zu verbessern.

4. Summary

In this dissertation, positron emission tomography (PET) was used to investigate cerebral amyloid distribution in terms of distribution pattern and longitudinal course, especially in patients with subsyndromal depression and SSRI therapy.

In the first part of the present dissertation, the relationship between striatal and cortical amyloid load was investigated to better understand the pattern of cerebral amyloid load spread and the regional cerebral connections. For this purpose, 73 amyloid-positive patients with neurodegenerative disease with a mean age of 71.5 ± 1.4 years were included. The neurodegenerative diseases included Alzheimer's dementia (AD, N = 34), mild cognitive impairment (MCI) due to AD (N = 26), frontotemporal lobar degeneration (N = 2), Parkinson's disease (N = 2), Lewy body dementia (N = 5), and patients with dementia symptoms of unclear etiology (N = 4). All patients received both glucose PET and amyloid PET examination with 11C-PiB of the brain.

For the 11C-PiB PET scans, an average dose of 555 ± 185 MBq of 11C-PiB was applied intravenously and images were acquired dynamically over 70 minutes from the time of application. For analysis, the PiB-PET images were co-registered to the individual FDG-PET images and then spatially normalized. Furthermore, the images were smoothed and normalized to the cerebellum. Based on this, voxel-wise analysis was performed using SPM8, and multiple regression was used to identify both possible positive and negative correlations.

The results revealed significant, exclusively positive correlations between striatal and cortical amyloid load, with the strongest correlation delineated frontobasally in the left Brodmann area 11. In contrast, no significant correlation could be found cerebellar.

Anatomical as well as functional connections are known between the striatal and cortical areas with significant correlation. This suggests that amyloid distribution in the brain follows functional and anatomical linkages. Future longitudinal studies may help to better understand the distribution patterns in the longitudinal course.

The second part of the thesis focuses on the influence of selective serotonin reuptake inhibitors (SSRI) on cognitive performance, gray matter atrophy, and amyloid load in patients with Alzheimer-type dementia or mild cognitive impairment at 2-year follow-up.

Preclinical studies suggested in a mouse model that SSRI administration may delay amyloidogenesis. Based on this hypothesis, we retrospectively examined the impact of SSRI therapy on cerebral amyloid load, cognitive performance, and gray matter atrophy in subsyndromal depressed patients with MCI or AD over a 2-year course. 256 patients from the ADNI database were studied, of whom 225 had MCI and 31 had AD-type dementia. These patients had both amyloid PET and MRI at baseline and 2-year follow-up. Furthermore, patients with depressive symptoms were subdivided into patients with (N = 24) and without (N = 49) SSRI medication, respectively.

The cognitive performance was shown using the difference in ADAS from baseline to follow-up. Amyloid deposition was quantified by amyloid PET with white matter as the reference region. In each case, analyses were performed including the covariates age, sex, years of education, ApoE4 status. Supplementary analyses were also performed in the subgroup of amyloid-positive patients.

Patients with depressive symptomatology receiving SSRI treatment showed a significantly lower decline in cognitive performance over the 2-year course compared with patients with depressive symptomatology who did not receive SSRI treatment. No

association with amyloid load at baseline was demonstrated. In the 2-year course, only suggested nonsignificant trends of a positive influence of SSRI medication on amyloid load could be shown.

The present results indicate that patients with mild cognitive impairment or AD benefit from SSRI therapy with respect to cognitive performance. The morphological correlate of this was lower gray matter atrophy rates in patients with SSRI treatment.

Because of the relatively small number of patients treated with SSRI for subsyndromal depression, our results suggest that increasing attention should be paid to adequate drug treatment of depressive symptomatology, even in the absence of manifest depression, in order to improve cognitive outcome.

5. Veröffentlichung I

Annals of Nuclear Medicine
https://doi.org/10.1007/s12149-018-1258-8

ORIGINAL ARTICLE

The correlation between striatal and cortical binding ratio of ^{11}C-PiB-PET in amyloid-uptake-positive patients

Julia Sauerbeck[1,2] · Kazunari Ishii[1,3,4] · Chisa Hosokawa[1,4] · Hayato Kaida[1] · Franziska T. Scheiwein[1,2] · Kohei Hanaoka[4] · Axel Rominger[2] · Matthias Brendel[2] · Peter Bartenstein[2] · Takamichi Murakami[1]

Received: 29 January 2018 / Accepted: 17 April 2018

Abstract

Purpose In subjects with amyloid deposition, striatal accumulation of ^{11}C-Pittsburgh compound B (PiB) demonstrated by positron emission tomography (PET) is related to the stage of Alzheimer's disease (AD). In this study, we investigated the correlation between striatal and cortical non-displaceable binding potential (BP_{ND}).

Methods Seventy-three subjects who complained of cognitive disturbance underwent dynamic PiB-PET studies and showed positive PiB accumulation were retrospectively selected. These subjects included 34 AD, 26 mild cognitive impairment, 2 frontotemporal lobar degeneration, 2 Parkinson's disease, 5 dementia with Lewy bodies, and 4 undefined diagnosis patients. Individual BP_{ND} images were produced from the dynamic data of the PiB-PET study, and voxel-based analyses were performed to estimate the correlations between striatal and other regional cortical BP_{ND} measures.

Results There were highly significant correlations between striatal and prefrontal BP_{ND}, with the highest correlation being demonstrated in left Brodmann area 11. We found that almost all of the high cortical BP_{ND} values correlated with striatal BP_{ND} values, with the exception of the occipital cortex with low correlation.

Conclusion Our study demonstrated positive correlations in amyloid deposits between the striatum and other cortical areas with functional and anatomical links. The amyloid distribution in the brain is not random, but spreads following the functional and anatomical connections.

Keywords Dementia · Alzheimer's disease · ^{11}C-PiB-PET · FDG-PET · Amyloid deposit · Striatum

Introduction

In this time of ageing populations, the number of patients with Alzheimer's disease (AD) and dementia is increasing, with a global total of 35.6 million in 2010, which is forecast to reach 66 million by 2030 [1]. As this implies an enormous burden on health care systems, much effort has been put into research on the pathophysiology of AD. It is known that AD is characterized by the presence of amyloid plaques and neurofibrillary tangles, as well as the significant loss of neurons [2–4].

To detect the pathology of AD, amyloid imaging tracers such as ^{11}C-Pittsburgh compound B (^{11}C-PiB) have been developed for in vivo PET imaging [5]. These tracers allow cerebral cortical accumulation to be shown in many patients with AD [6] and other AD-related diseases. ^{11}C-PiB is a thioflavin-T derivative with a small molecular size that is able to bind to amyloid proteins [5, 7, 8]. Amyloid accumulation in dementia subjects is mainly apparent in the posterior parietal regions, precuneus, and frontal cortex [9]. Not only cortical, but also striatal uptake of ^{11}C-PiB has been observed in AD patients, with a robust correlation being found between amyloid deposits in the ventral striatum and the medial part of the orbitofrontal area [10].

✉ Kazunari Ishii
ishii@med.kindai.ac.jp

1 Department of Radiology, Kindai University Faculty of Medicine, 377-2 Ohnohigashi, Osakasayama, Osaka 589-8511, Japan

2 Department of Nuclear Medicine, Ludwig-Maximilians-University of Munich, Munich, Germany

3 Neurocognitive Disorders Center, Kindai University Hospital, Osakasayama, Osaka, Japan

4 Division of Positron Emission Tomography, Institute of Advanced Clinical Medicine, Kindai University, Osakasayama, Osaka, Japan

Published online: 05 May 2018

Previously, we reported that PiB-accumulation-positive subjects with high striatal PiB uptake have an increased mean cortical standard uptake value ratio (SUVR) in comparison with PiB-positive subjects without striatal uptake, suggesting that high amyloid deposition in the striatum is linked to amyloid deposition within the frontal region, which may occur later in the course of AD progression [11]. In this study, we aimed to further investigate this connectivity between striatal and regional cortical PiB uptake: amyloid pathology, using non-displaceable binding potential (BP_{ND}) images obtained from ^{11}C-PiB-PET with dynamic scanning; these reflect the clear binding of PiB tracer in equivocal PiB accumulation subjects [12].

Materials and methods

Patient population

This retrospective study included 73 patients (31 men and 42 women; mean age ± SD, 71.5 ± 2.1 years; mean Mini-Mental State Examination score, 21.7 ± 1.4) who underwent both an ^{11}C-PiB dynamic PET study and a 2-deoxy-2-[13] fluoro-D-glucose (FDG)-PET study. All of the subjects with amyloid positive deposition were selected from those included in the previous study by Scheiwein et al. [11]. Amyloid positive deposition (PiB-positive) was evaluated in four cortical regions, including bilateral frontal, parietal, and temporal lobes, and bilateral precuneus/posterior cingulate gyri. PiB-positive images were defined as those having higher accumulation in the cerebral cortex than in the white matter (non-specific accumulation area) and PiB-negative images were defined as those having no cortical accumulation [11]. The 73 subjects included 34 with AD (46.6%), 26 with mild cognitive impairment (MCI) due to AD (35.6%), 2 with frontotemporal lobar degeneration (2.7%), 2 with Parkinson's disease (2.7%), 5 with Lewy body disease (6.8%), and 4 with no clear diagnosis (5.5%) after 2 year follow-up. The diagnostic criteria of the Neurological and Communicative Disorders and Stroke–Alzheimer's Disease and Related Disorders Association for AD [14] were used to assess the patients, as well as the third report of the Dementia with Lewy Bodies Consortium for DLB [15]. The subjects with mild cognitive impairment and frontotemporal lobar degeneration fulfilled the published criteria [16, 17]. All subjects underwent ^{18}F-FDG-PET scanning within 1–175 days (mean, 15.2 days; median, 12 days) of the ^{11}C-PiB-PET scanning. The institutional ethics committee approved this study, and all subjects or guardians signed a written informed consent form.

Data acquisition

The ^{11}C-PiB-PET and ^{18}F-FDG-PET data acquisitions were similar to those described in a previous study [18, 19]. PET scans were performed on a PET scanner (ECAT Accel; Siemens AG; Erlangen, Germany) in 3-dimensional mode. The ^{11}C-PiB data were continuously acquired for 70 min after intravenous administration of 555 ± 185 MBq of ^{11}C-PiB. For ^{18}F-FDG-PET, the subjects were instructed to fast for at least 4 h prior to the scan and they were asked to lie quietly in a dimly lit room with their eyes open and minimal sensory stimulation. A 30-min emission scan was acquired, starting 30 min after intravenous injection of 185 MBq of ^{18}F-FDG.

Image processing

The BP_{ND} images were analysed with the PMOD software package (version 3.308; PMOD Technologies Ltd., Zürich, Switzerland), using the full set of dynamic data (0–70 min after injection). Parametric images of regional ^{11}C-PiB uptake (BP_{ND} images) were generated using Logan graphical analysis, with reference to the cerebellar cortex [20]. This time we used reference Logan graphical analysis without the k2 at the reference region with the PMOD software.

Statistical analysis

Voxelwise analyses were performed by co-registering the PiB-PET images to the individual FDG-PET images using the statistical parametric mapping software (SPM8: Wellcome Trust Centre for Neuroimaging, University College London, London, UK; http://www.fil.ion.ucl.ac.uk/spm/software/spm8/). First, individual's BP_{ND} images were co-registered to their FDG-PET image. Next, the FDG-PET image was spatially normalised to the Montreal Neurologic Institute standard-space template (MNI space). Following this, the BP_{ND} images were also spatially normalised, using the individual transform from the FDG-PET spatial normalisation.

All BP_{ND} and FDG-PET images were smoothed with an isotropic 8 mm Gaussian kernel to increase the signal-to-noise ratio and compensate for differences in gyral anatomy between individuals. Individual FDG images were normalised by the global FDG uptake, while the individual BP_{ND} values were normalised by the cerebellar BP_{ND} values.

Voxelwise analysis using SPM8 was performed to find regional correlations between striatal and cortical BP_{ND}.

This involved a multiple regression to assess both positive and negative correlations. A p value of less than 0.05 familywise error corrected (FWE) for multiple comparisons was considered to be statistically significant.

Results

The voxelwise analyses using multiple regression showed significant positive correlations but no negative ones. A comparison of striatal and cortical BP_{ND} values revealed a highly significant correlation between the striatum and prefrontal cortex. The highest correlation with striatal values occurred in the left Brodmann area (BA) 11 ($p<0.05$ FWE corrected), with the MNI coordinates of the peak level voxel being $x=-5$ mm, $y=38$ mm, and $z=-10$ mm ($t=17.58$). The right BA11 also showed a strong correlation with striatal values. Further strong correlations were also found with bilateral BA 32, 9, and 10. The significant results are listed in detail (BA, MNI coordinates, and t values) in Table 1. Figure 1 shows that almost all of the cortical BP_{ND} values correlated with striatal BP_{ND} values, with the exception of the cerebellar BP_{ND} value. The strongest correlation in the basal frontal area is demonstrated by a dark red colour overlaid onto a rendered MR image. Correlations with the occipital cortices were low.

Representative case (Fig. 2): A 72-year-old male with AD, his MMSE score is 19. BP_{ND} of the left striatum is larger than that of the right striatum. They are correlated with each frontal $BP_{ND,}$ but are not correlated with each temporal BP_{ND}: the left frontal BP_{ND} is larger than the right frontal BP_{ND}, though the left temporal BP_{ND} is smaller than the right temporal BP_{ND}. The precuneus BP_{ND} is also correlated with striatum BP_{ND}, but the accumulation in the precuneus is larger than that in the striatum or in the frontal lobe.

Discussion

Several studies have revealed an increased uptake of ^{11}C-PiB in AD, not only in cortical areas such as the posterior cingulate and frontal, parietal, and lateral temporal cortices, but also in the striatum [21, 22]. There is a specific chronological order of amyloid-beta (Abeta) deposition in the brain.

Table 1 Statistically significant correlations between striatal and cortical binding potential

Brodmann area	Brain region	Side	Coordinates			t values
			X	Y	Z	
BA 11	Orbitofrontal cortex	l	−9	33	−9	17.49
BA 11	Orbitofrontal cortex	r	1	26	−12	16.80
BA 32	Dorsal anterior cingulate cortex (DACC)	l	−8	35	11	15.46
BA 32	Dorsal anterior cingulate cortex (DACC)	r	11	37	7	15.24
BA 45	Broca's area	r	32	25	6	14.43
BA 9	Dorsolateral/ medial prefrontal cortex	l	−37	21	25	14.26
BA 9	Dorsolateral/ medial prefrontal cortex	r	37	28	24	14.15
BA 46	Dorsolateral prefrontal cortex (DLPFC)	r	37	39	13	14.10
BA 31	Dorsal posterior cingulate	l	−11	−55	29	14.09
BA 10	Prefrontal cortex	l	−33	43	3	13.88
BA 10	Prefrontal cortex	r	7	46	−11	13.46

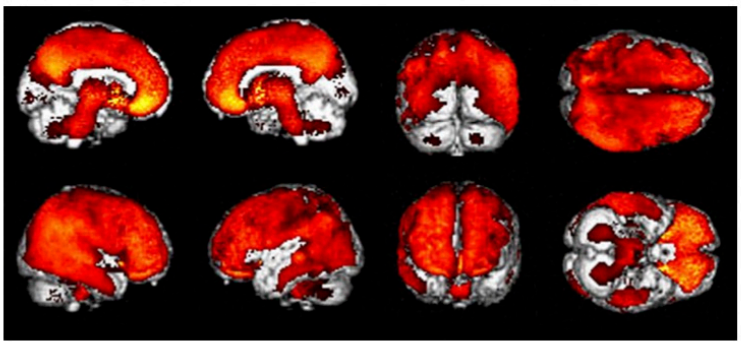

Fig. 1 Significant correlations in the BP_{ND} of the striatum and cortical areas

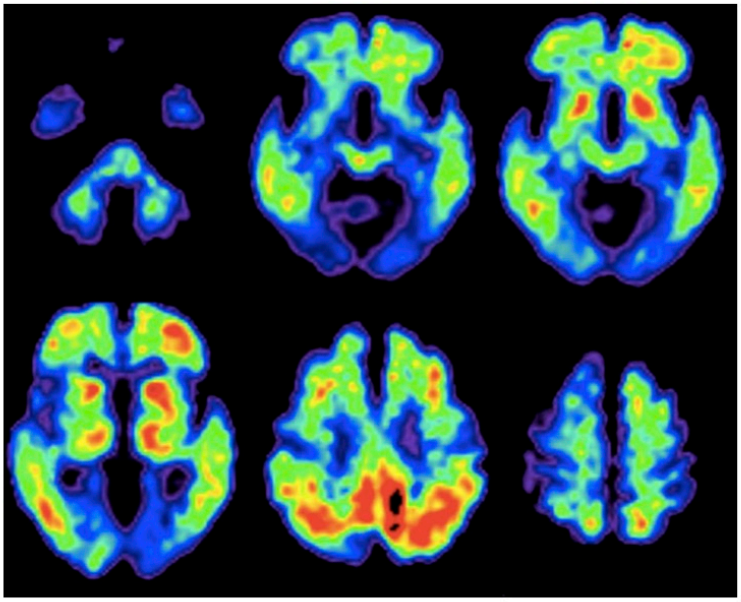

Fig. 2 Representative BP_{ND} image of a patient with Alzheimer disease. Each unilateral striatum BP_{ND} is correlated with each frontal BP_{ND} but not correlated with each temporal BP_{ND}. Bilateral precuneus BP_{ND} is also correlated with each striatum BP_{ND}, but the uptake in the precuneus is larger than that in the striatum or frontal lobe

At first, Abeta deposition is found in the neocortex, with allocortical brain regions becoming additionally involved later on, before the third of five phases, where the deposition expands into the striatum [23]. Early stages may not, therefore, show an increased uptake of PiB, but the more advanced the beta-amyloidosis is, the more likely it is that the striatum is affected, in addition to the cortical regions. Given this background, our study set out to investigate the connections between striatal and cortical BP_{ND}.

A similar study by Ishibashi et al. aimed to examine the striatal distribution pattern of PiB-SUVR in detail, while, furthermore, looking for a correlation between striatal and cortical uptake [10]. However, while they used SPSS and static ^{11}C-PiB images (SUVR images) for the voxel-based analysis, our study used voxel-based analysis with BP_{ND} images, which reflect amyloid deposition more accurately than SUVR images. This time we used Logan plot analysis for BP_{ND} images, because we thought that it is as optimal as other analysis methods, however, Yaqub et al. reported that receptor parametric mapping (RPM)2 and multi-linear reference tissue models (MRTM)2 in their study were provided with the best accuracy and precision in the simulation studies and are, therefore, the methods of choice for parametric analysis of clinical ^{11}C- PiB studies [24]. Using Logan plot analysis, noise in tissue time activity curve (tTAC) leads to underestimating the estimated distribution volume [25]. ROI analysis can reduce the noise in tTAC, but it cannot make analysis of the whole brain regions; therefore, we used voxel-by-voxel Logan graphical analysis. Therefore, this study with Logan plot analysis may have a limitation and we would like to entrust further study using better analysis as Yaqub et al. suggest.

Ishibashi et al. found the highest SUVR in the ventral striatum, and this strongly correlated with PiB uptake in the medial part of the orbitofrontal area, a region corresponding to BA 11 and 12. We also found that the two strongest correlations occurred between the striatum and the left and right BA 11. This brain area participates in learning mechanisms, especially distinction learning [26]. Even though the connections between the orbitofrontal cortex (OFC) and striatum are still not fully understood, there are a number of studies that have investigated them. It is believed that there is an anterograde distribution into areas that receive neuronal input from those areas that are already affected by Abeta deposition [23]. Corresponding to this finding, the striatum receives input from the OFC, as previously revealed by a rat study [27]. According to the study, the OFC has an important role in making decisions on the biological significance of associative information, while the input of the hippocampus may remain unfiltered. The OFC also has an important role in stimulus-reward learning [28].

The striatum has been shown to be essential for decision-making [29]. As both the striatum and orbitofrontal cortex play a major role in decision-making [30], this task may be an important aspect of the relationship between the striatum and orbitofrontal cortex. Furthermore, the

dorsolateral prefrontal cortex (BA 46) is also important for decision-making, and correlates significantly with the amyloid load of the striatum [31]. Several studies have shown that decision-making is impaired in people diagnosed with MCI, while this is even more so in AD patients [32]. Therefore, the clinical symptoms of dementia correspond with our finding of a significant correlation between the striatum and cortical areas, which are responsible for decision-making.

Another highly significant correlation was found between bilateral BA 32 and the striatum (Table 1). BA 32 is also part of the prefrontal cortex, and represents the dorsal anterior cingulate. The anterior cingulate cortex (ACC) shows reduced glucose metabolism in depressed individuals [33], and therefore, it is assumed to be vulnerable to depression [34]. A previous study found close links between the ACC and striatum in depressed patients, including significant functional connectivity (measured using functional magnetic resonance imaging) between the ACC and striatum, as well as orbitofrontal cortex [35]. This further strengthens our reasoning that the strong correlation between cortical amyloid accumulation and striatal amyloid deposition is not random, but reflects functionally related areas.

Furthermore, we detected a significant correlation between striatal BP_{ND} and BP_{ND} in the right BA 45. This area represents Broca's area, the centre of speech, and language production [36].

Other significant correlations were found between the striatum, and bilateral BA 9 and 10 in the prefrontal cortex. This part of the prefrontal cortex appears to play a part in idiomatic sentence processing [37] and remembrance of the past experiences [38].

BA 31 (part of the posterior cingulate cortex) is important for cognition, and probably also has a role in controlling attentional focus [39]. As the striatum plays an important role in cognitive functioning [40, 41], the significant correlation between BA 31 and the striatum may reflect a connection between these two areas of the brain.

This study has some limitations. First, various types and stages of dementia were included. It is difficult to find typical patterns for one disease, e.g., AD; however, the study does show general correlations in patients with dementia. Furthermore, as Ishibashi et al. [10] demonstrated, there appear to be different connections, depending on the area of the striatum. As we did not distinguish between different areas of the striatum, we only could find significant correlations with respect to the whole striatal amyloid load, not with regard to intra-striatal differences. Further studies to reveal the fine details of how the functional and anatomical networks vary between each region of the striatum and cortex will, therefore, be helpful.

Conclusions

Our study found several positive correlations between the striatum and cortical areas with functional and anatomical links to the striatum. We, therefore, think that the amyloid distribution in the brain is not random, but depends on, and may spread because of, the functional and anatomical connections.

References

1. Wortmann M. Dementia: a global health priority—highlights from an ADI and World Health Organization report. Alzheimers Res Ther. 2012;4:40. https://doi.org/10.1186/alzrt143.
2. Price JL, Morris JC. Tangles and plaques in nondemented aging and "preclinical" Alzheimer's disease. Ann Neurol. 1999;45:358 – 68.
3. Braak H, Braak E. Neuropathological stageing of Alzheimer-related changes. Acta Neuropathol. 1991;82:239–59.
4. Mirra SS, Heyman A, McKeel D, Sumi SM, Crain BJ, Brownlee LM, et al. The consortium to establish a registry for Alzheimer's disease (CERAD). Part II. Standardization of the neuropathologic assessment of Alzheimer's disease. Neurology. 1991;41:479–86.
5. Mathis CA, Wang Y, Holt DP, Huang GF, Debnath ML, Klunk WE. Synthesis and evaluation of 11C-labeled 6-substituted 2-arylbenzothiazoles as amyloid imaging agents. J Med Chem. 2003;46:2740–54. https://doi.org/10.1021/jm030026b.
6. Hatsuta H, Takao M, Ishii K, Ishiwata K, Saito Y, Kanemaru K, et al. Amyloid beta accumulation assessed with (1)(1)C-Pittsburgh compound B PET and postmortem neuropathology. Curr Alzheimer Res. 2015;12:278–86.
7. Leinonen V, Alafuzoff I, Aalto S, Suotunen T, Savolainen S, Nagren K, et al. Assessment of beta-amyloid in a frontal cortical brain biopsy specimen and by positron emission tomography with carbon 11-labeled Pittsburgh Compound B. Arch Neurol. 2008;65:1304–9. https://doi.org/10.1001/archneur.65.10.noc80013.
8. Ikonomovic MD, Klunk WE, Abrahamson EE, Mathis CA, Price JC, Tsopelas ND, et al. Post-mortem correlates of in vivo PiB-PET amyloid imaging in a typical case of Alzheimer's disease. Brain. 2008;131:1630–45. https://doi.org/10.1093/brain/awn016.
9. Buckner RL, Snyder AZ, Shannon BJ, LaRossa G, Sachs R, Fotenos AF, et al. Molecular, structural, and functional characterization of Alzheimer's disease: evidence for a relationship between default activity, amyloid, and memory. J Neurosci. 2005;25:7709–17. https://doi.org/10.1523/JNEUROSCI.2177-05.2005.
10. Ishibashi K, Ishiwata K, Toyohara J, Murayama S, Ishii K. Regional analysis of striatal and cortical amyloid deposition in patients with Alzheimer's disease. Eur J Neurosci. 2014;40:2701–6. https://doi.org/10.1111/ejn.12633.
11. Scheiwein TF, Ishii K, Hosokawa C, Kaida H, Hyodo T, Hanaoka K, et al. Regional differences in amyloid deposition between 11C-PiB PET positive patients with and without elevated striatal amyloid uptake. J Alzheimer Dis Parkinsonism. 2017;7:317. https://doi.org/10.4172/2161-0460.1000317.
12. Hosokawa C, Ishii K, Kimura Y, Hyodo T, Hosono M, Sakaguchi K, et al. Performance of 11C-pittsburgh compound B PET binding potential images in the detection of amyloid deposits on equivocal static images. J Nucl Med. 2015;56:1910–5. https://doi.org/10.2967/jnumed.115.156414.

13. Calcagni ML, Lavalle M, Mangiola A, Indovina L, Leccisotti L, De Bonis P, et al. Early evaluation of cerebral metabolic rate of glucose (CMRglu) with 18F-FDG PET/CT and clinical assessment in idiopathic normal pressure hydrocephalus (INPH) patients before and after ventricular shunt placement: preliminary experience. Eur J Nucl Med Mol Imaging. 2012;39:236 – 41. https://doi.org/10.1007/s00259-011-1950-6.
14. McKhann G, Drachman D, Folstein M, Katzman R, Price D, Stadlan EM. Clinical diagnosis of Alzheimer's disease: report of the NINCDS-ADRDA work group under the auspices of Department of Health and Human Services task force on Alzheimer's disease. Neurology. 1984;34:939–44.
15. McKeith IG, Dickson DW, Lowe J, Emre M, O'Brien JT, Feldman H, et al. Diagnosis and management of dementia with Lewy bodies: third report of the DLB Consortium. Neurology. 2005;65:1863–72. https://doi.org/10.1212/01.wnl.0000187889.17253.b1.
16. Neary D, Snowden JS, Gustafson L, Passant U, Stuss D, Black S, et al. Frontotemporal lobar degeneration: a consensus on clinical diagnostic criteria. Neurology. 1998;51:1546–54.
17. Petersen RC, Doody R, Kurz A, Mohs RC, Morris JC, Rabins PV, et al. Current concepts in mild cognitive impairment. Arch Neurol. 2001;58:1985–92.
18. Hosokawa C, Ishii K, Hyodo T, Sakaguchi K, Usami K, Shimamoto K, et al. Investigation of (11)C-PiB equivocal PET findings. Ann Nucl Med. 2015;29:164–9. https://doi.org/10.1007/s12149-014-0924-8.
19. Ishii K, Hosokawa C, Hyodo T, Sakaguchi K, Usami K, Shimamoto K, et al. Regional glucose metabolic reduction in dementia with Lewy bodies is independent of amyloid deposition. Ann Nucl Med. 2015;29:78–83. https://doi.org/10.1007/s12149-014-0911-0.
20. Logan J, Fowler JS, Volkow ND, Wang GJ, Ding YS, Alexoff DL. Distribution volume ratios without blood sampling from graphical analysis of PET data. J Cereb Blood Flow Metab. 1996;16:834–40. https://doi.org/10.1097/00004647-199609000-00008.
21. Kemppainen NM, Aalto S, Wilson IA, Nagren K, Helin S, Bruck A, et al. Voxel-based analysis of PET amyloid ligand [11C]PIB uptake in Alzheimer disease. Neurology. 2006;67:1575–80. https://doi.org/10.1212/01.wnl.0000240117.55680.0a.
22. Klunk WE, Engler H, Nordberg A, Wang Y, Blomqvist G, Holt DP, et al. Imaging brain amyloid in Alzheimer's disease with Pittsburgh Compound-B. Ann Neurol. 2004;55:306–19. https://doi.org/10.1002/ana.20009.
23. Thal DR, Rub U, Orantes M, Braak H. Phases of A beta-deposition in the human brain and its relevance for the development of AD. Neurology. 2002;58:1791–800.
24. Yaqub M, Tolboom N, Boellaard R, van Berckel BN, van Tilburg EW, Luurtsema G, et al. Simplified parametric methods for [11C]PIB studies. NeuroImage. 2008;42:76–86. https://doi.org/10.1016/j.neuroimage.2008.04.251.
25. Kimura Y, Naganawa M, Shidahara M, Ikoma Y, Watabe H. PET kinetic analysis—pitfalls and a solution for the Logan plot. Ann Nucl Med. 2007;21:1–8.
26. Gottfried JA, Dolan RJ. Human orbitofrontal cortex mediates extinction learning while accessing conditioned representations of value. Nat Neurosci. 2004;7:1144–52. https://doi.org/10.1038/nn1314.
27. Cooch NK, Stalnaker TA, Wied HM, Bali-Chaudhary S, McDannald MA, Liu TL, et al. Orbitofrontal lesions eliminate signalling of biological significance in cue-responsive ventral striatal neurons. Nat Commun. 2015;6:7195. https://doi.org/10.1038/ncomms8195.
28. Rolls ET, Hornak J, Wade D, McGrath J. Emotion-related learning in patients with social and emotional changes associated with frontal lobe damage. J Neurol Neurosurg Psychiatry. 1994;57:1518–24.
29. Burton AC, Bissonette GB, Lichtenberg NT, Kashtelyan V, Roesch MR. Ventral striatum lesions enhance stimulus and response encoding in dorsal striatum. Biol Psychiatry. 2014;75:132–9. https://doi.org/10.1016/j.biopsych.2013.05.023.
30. Wallis JD. Orbitofrontal cortex and its contribution to decision-making. Annu Rev Neurosci. 2007;30:31–56. https://doi.org/10.1146/annurev.neuro.30.051606.094334.
31. Yamamoto DJ, Woo CW, Wager TD, Regner MF, Tanabe J. Influence of dorsolateral prefrontal cortex and ventral striatum on risk avoidance in addiction: a mediation analysis. Drug Alcohol Depend. 2015;149:10–7. https://doi.org/10.1016/j.drugalcdep.2014.12.026.
32. de Siqueira AS, Yokomizo JE, Jacob-Filho W, Yassuda MS, Aprahamian I. Review of decision-making in game tasks in elderly participants with Alzheimer Disease and mild cognitive impairment. Dement Geriatr Cogn Disord. 2017;43:81–8. https://doi.org/10.1159/000455120.
33. Drevets WC. Neuroimaging and neuropathological studies of depression: implications for the cognitive-emotional features of mood disorders. Curr Opin Neurobiol. 2001;11:240–9.
34. Vogt BA, Vogt L, Farber NB, Bush G. Architecture and neurocytology of monkey cingulate gyrus. J Comp Neurol. 2005;485:218–39. https://doi.org/10.1002/cne.20512.
35. Davey CG, Harrison BJ, Yucel M, Allen NB. Regionally specific alterations in functional connectivity of the anterior cingulate cortex in major depressive disorder. Psychol Med. 2012;42:2071–81.
36. Trupe LA, Varma DD, Gomez Y, Race D, Leigh R, Hillis AE, et al. Chronic apraxia of speech and Broca's area. Stroke. 2013;44:740–4. https://doi.org/10.1161/STROKEAHA.112.678508.
37. Lauro LJ, Tettamanti M, Cappa SF, Papagno C. Idiom comprehension: a prefrontal task? Cereb Cortex. 2008;18:162–70. https://doi.org/10.1093/cercor/bhm042.
38. Lepage M, Ghaffar O, Nyberg L, Tulving E. Prefrontal cortex and episodic memory retrieval mode. Proc Natl Acad Sci USA. 2000;97:506–11.
39. Leech R, Sharp DJ. The role of the posterior cingulate cortex in cognition and disease. Brain. 2014;137:12–32. https://doi.org/10.1093/brain/awt162.
40. Nakano K, Kayahara T, Tsutsumi T, Ushiro H. Neural circuits and functional organization of the striatum. J Neurol. 2000;247(Suppl 5):V1-15.
41. Yang YK, Yao WJ, McEvoy JP, Chu CL, Lee IH, Chen PS, et al. Striatal dopamine D2/D3 receptor availability in male smokers. Psychiatry Res. 2006;146:87–90. https://doi.org/10.1016/j.pscychresns.2005.09.008.

6. Veröffentlichung II

Journal of Alzheimer's Disease 65 (2018) 793–806
DOI 10.3233/JAD-170387
IOS Press

Serotonin Selective Reuptake Inhibitor Treatment Improves Cognition and Grey Matter Atrophy but not Amyloid Burden During Two-Year Follow-Up in Mild Cognitive Impairment and Alzheimer's Disease Patients with Depressive Symptoms

Matthias Brendel[a,1], Julia Sauerbeck[a,1], Sonja Greven[b], Sebastian Kotz[a], Franziska Scheiwein[a], Janusch Blautzik[a], Andreas Delker[a], Oliver Pogarell[c], Kazunari Ishii[d], Peter Bartenstein[a], Axel Rominger[a,e,*] and for the Alzheimer's Disease Neuroimaging Initiative[2]
[a]*Department of Nuclear Medicine, University of Munich, Germany*
[b]*Department of Statistics, University of Munich, Germany*
[c]*Department of Psychiatry, University of Munich, Germany*
[d]*Department of Radiology, Kindai University Faculty of Medicine, Osakasayama City, Osaka, Japan*
[e]*Department of Nuclear Medicine, Inselspital, University Hospital Bern, Switzerland*

Accepted 30 May 2018

Abstract. Late-life depression, even when of subsyndromal severity, has shown strong associations with mild cognitive impairment (MCI) and Alzheimer's disease (AD). Preclinical studies have suggested that serotonin selective reuptake inhibitors (SSRIs) can attenuate amyloidogenesis. Therefore, we aimed to investigate the effect of SSRI medication on amyloidosis and grey matter volume in subsyndromal depressed subjects with MCI and AD during an interval of two years. 256 cognitively affected subjects (225 MCI/ 31 AD) undergoing [^{18}F]-AV45-PET and MRI at baseline and 2-year follow-up were selected from the ADNI database. Subjects with a positive depression item (DEP(+); $n=73$) in the Neuropsychiatric Inventory Questionnaire were subdivided to those receiving SSRI medication (SSRI(+); $n=24$) and those without SSRI treatment (SSRI(–); $n=49$). Longitudinal cognition (Δ-ADAS), amyloid deposition rate (standardized uptake value, using white matter as reference region ($SUVR_{WM}$), and changes in grey matter volume were compared using common covariates. Analyses were performed separately in all subjects and in the subgroup of amyloid-positive subjects. Cognitive performance in DEP(+)/SSRI(+) subjects (Δ-ADAS: –5.0%) showed less deterioration with 2-year follow-up when compared to

[1]These authors contributed equally to this work.

[2]Data used in preparation of this article were obtained from the Alzheimer's Disease Neuroimaging Initiative (ADNI) database (http://adni.loni.usc.edu). As such, the investigators within the ADNI contributed to the design and implementation of ADNI and/or provided data but did not participate in analysis or writing of this report. A complete listing of ADNI investigators can be found at: http://adni.loni.usc.edu/wp-content/uploads/how_to_apply/ADNI_Acknowledgement_List.pdf

*Correspondence to: Prof. Dr. Axel Rominger, MD, Department of Nuclear Medicine, University of Bern, Switzerland. Tel.: +41 32 632 26 10; Fax: +41 32 632 76 63; E-mail: axel.rominger@insel.ch.

DEP(+)/SSRI(–) subjects (Δ-ADAS: +18.6%, $p < 0.05$), independent of amyloid $SUVR_{WM}$ at baseline. With SSRI treatment, the progression of grey matter atrophy was reduced (–0.9% versus –2.7%, $p < 0.05$), notably in fronto-temporal cortex. A slight trend towards lower amyloid deposition rate was observed in DEP(+)/SSRI(+) subjects versus DEP(+)/SSRI(–). Despite the lack of effect to amyloid PET, SSRI medication distinctly rescued the declining cognitive performance in cognitively affected patients with depressive symptoms, and likewise attenuated grey matter atrophy.

Keywords: Alzheimer's disease, amyloid PET, depressive symptoms, grey matter volume, SSRI

INTRODUCTION

Multiple studies have revealed that late-life depression is associated with increased risk for mild cognitive impairment (MCI) [1, 2] and Alzheimer's disease (AD) [2, 3]. Furthermore, there is evidence that co-morbid subsyndromal depression has significant detrimental effects on disability in MCI patients assessed with the Functional Assessment Questionnaire [4], which emphasizes the need for addressing depression in geriatric health care programs, even when occurring at subsyndromal severity.

With the development of [^{18}F]-fluorinated positron emission tomography (PET) ligands for amyloid-β (Aβ-PET), there has emerged a greater understanding of the progression of AD pathology [5, 6]. Individuals can be subdivided into Aβ positive (Aβ+) or negative (Aβ–) groups even at an early disease stage before the onset of frank clinical symptoms of dementia [7]. This innovation led to multiple investigations aiming to enlighten the link between depressive symptoms and AD pathology by measuring non-invasively the amyloid burden in brain of patients with cognitive symptoms. Wu and colleagues found that a lifetime history of major depression is associated with increased amyloid burden in the brain of healthy individuals (HC) [8], and that patients with comorbidity of major depression and MCI have greater amyloid burden when compared to age-matched major depression patients [9].

We earlier found that Aβ(+) subjects with MCI and concurrent subsyndromal depression showed a higher fronto-temporal amyloid load and a faster conversion to AD than did non-depressed MCI individuals [10]. The converse relationship may also hold; others observed a 4.5-fold increased risk in healthy controls for developing depressive symptoms during a 4-year observation period when amyloid pathology was present in the brain at baseline [11]. However, there are also findings not supporting an association between cortical amyloid burden, cognitive dysfunction, and depressive symptoms in MCI and AD patients [12].

The generally accepted link between depression, amyloid pathology, and progression of dementia raises the important question of whether dementia symptoms could potentially be ameliorated by treatment with antidepressants. A very recent meta-analysis including only the small number of relatively low-powered studies in patients with dementia indicated neither cognitive benefit nor harm from treatment with serotonin selective reuptake inhibitors (SSRIs) [13]; the authors emphasized the need for sufficiently powered studies of this intervention strategy. Given the clinical heterogeneity of geriatric depression [14], well-designed, large-scale amyloid PET imaging studies might be suitable to clarify the association between depression, amyloid pathology, and therapeutic effects of SSRI treatment [15]. Intriguingly, lower amyloid burden was observed by [^{11}C]-PiB PET in healthy controls with a history of SSRI intake when compared to SSRI-naive control subjects [16]. Importantly, that cross-sectional investigation also found a negative correlation between amyloid burden and duration of previous SSRI intake. In support of a causal relationship, a recent preclinical study of prospective design revealed that treatment with the SSRI citalopram arrested further growth of pre-existing plaques and inhibited new plaque formation by 78% in aged transgenic AD mice [17].

Given this background, we aimed to investigate the influence of SSRIs use on longitudinal neuroimaging findings of amyloid load and brain volume in conjunction with cognitive assessment. Therefore, we analyzed longitudinal Aβ-PET data over a 2-year period in MCI or AD individuals with either presence or absence of depressive symptoms, and documentation of SSRI treatment.

MATERIAL AND METHODS

Alzheimer's disease neuroimaging initiative

Data used in the preparation of this article were obtained from the Alzheimer's Disease

Neuroimaging Initiative (ADNI) database (http://adni.loni.usc.edu). The ADNI was launched in 2003 as a public-private partnership, led by Principal Investigator Michael W. Weiner, MD. The primary goal of ADNI has been to test whether serial magnetic resonance imaging (MRI), positron emission tomography (PET), other biological markers, and clinical and neuropsychological assessment can be combined to measure the progression of MCI and early AD. Data from ADNI-GO/-2 were included in this work as available on March 3, 2015. ADNI-GO contains 700 subjects, of whom 200 showed the mildest symptomatic phase of AD (EMCI). 500 are healthy controls, together with MCI patients from the ADNI1 collective. The ADNI-2 dataset consists of 1350 subjects, consisting of the 700 subjects of the ADNI-GO dataset with addition of 150 new normal controls, 150 new early MCI cases, and 200 late MCI and mild AD patients.

Patient selection and study design

On the database cut-off date, 409 subjects in total with either healthy cognition (HC), MCI, or AD diagnosis had received [^{18}F]-AV45 PET and T1w MRI at baseline and 2-year follow-up (24 ± 2.5 months) within ADNI-GO/ADNI-2. The discrimination between HC, MCI, and AD was made following the Mini-Mental State Examination (MMSE; score 0–30) as well as the Clinical Dementia Rating (CDR; score 0–3) and clinical criteria. MMSE from 24 to 30 and CDR of 0 are defined as HC, MMSE from 24 to 30 and CDR of 0.5 plus objective memory loss and preserved activities of the daily living were designated as MCI. Patients with diagnosis of AD show MMSE of 20–26, CDR of 0.5 to 1.0, and otherwise meet the NINCDS/ADRDA criteria for probable AD.

Apolipoprotein E4 (ApoE4) status was compiled together with gender and education level (years), while age, NPI-Q score, Assessment Scale (ADAS; score 0–70), and Mini Mental State Examination (MMSE; score 0–30) were recorded at the time of the PET scans.

All subjects were stratified in the following groups:

A) Dementia symptoms: According to the diagnosis at baseline, all subjects were divided into cognitively affected (MCI or AD) and unaffected subjects (HC). The group of MCI and AD was further divided according to the two following subgroups on the basis of depression symptoms.

B) Depressive symptoms: Subsyndromal depression was diagnosed in accordance with item #4 (depressive symptoms) of the NPI-Q [18] at the time of the baseline PET scan. A positive score on item #4 indicated depressive symptoms (DEP(+)), and negative indicated absence of depressive symptoms (DEP(–)).

C) SSRI medication: Longitudinal 2-year SSRI treatment was assessed from the medication file in the ADNI documentation, while individual dosage was not considered. All subjects receiving SSRI treatment at baseline and follow-up without discontinuation of the drug were considered as treated (SSRI(+)), whereas all other subjects were categorized as non-treated (SSRI(–)).

According to the categories named above, the following three subcategories were examined (in brackets there are the numbers of MCI-/AD-cases):

I. DEP(+)/SSRI(+) $n = 24$ (MCI: $n = 22$ (91.7%); AD: $n = 2$ (8.3%))
II. DEP(+)/SSRI(–) $n = 49$ (MCI: $n = 42$ (85.7%); AD: $n = 7$ (14.3%))
III. DEP(–) $n = 183$ (MCI: $n = 161$ (88.0%); AD: $n = 22$ (12.0%))

D) Brain amyloid burden: All PET analyses were performed separately in all subjects and likewise in the subgroup of Aβ(+) subjects, aiming to score the presence of significant AD-typical amyloid burden in relation to newly proposed diagnosis criteria [19]. Aβ(+) and Aβ(–) [^{18}F]-AV45-PET status was defined in accordance with our calculated threshold of 0.77 for the standardized uptake value ratio (SUVR). For the SUVR calculation, individual gray matter VOIs of frontal, parietal, temporal and precuneal/posterior cingulate gyrus were summed to form a composite (COMP) VOI. The SUVR then was calculated by dividing the mean COMP SUV by the mean reference SUV of the white matter, as this reference region is previously shown to provide the highest discrimination between HC and AD for this tracer [20]. Figure 1 illustrates the study design.

Image data

ADNI [^{18}F]-AV45-PET acquisition and pre-processing

The [^{18}F]-AV45-PET images had been acquired using Siemens, GE, and Philips PET scanners according to a standard dynamic 50–70 min protocol following the intravenous injection of 370 ± 37 MBq of [^{18}F]-AV45. Data were corrected for both scatter and measured attenuation, which was determined using the CT scan for PET/CT scanners, or a transmis-

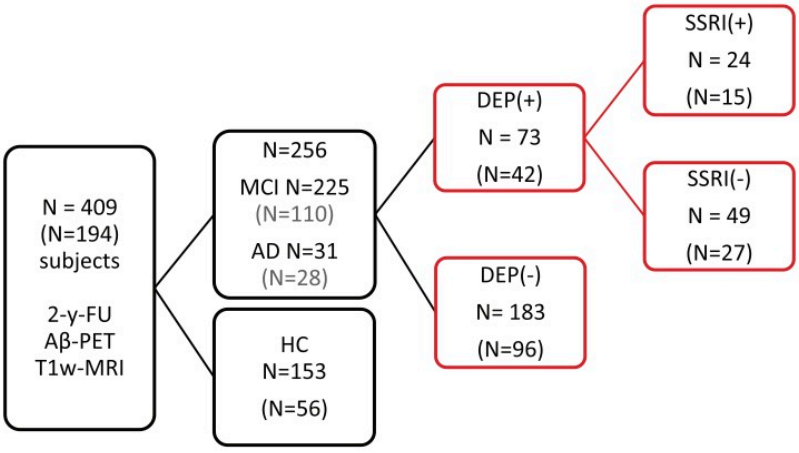

Fig. 1. Stratification of 409 subjects with [^{18}F]-AV45-PET and T1w MRI at baseline- and 2-year-follow-up-PET scan. The numbers of Aβ(+) subjects for each group are indicated in brackets. All subjects were first categorized according to their diagnosis as MCI, AD and HC subjects. Subsequently, the NPI-Q was used to subdivide the MCI and AD group into subsyndromal depressed (DEP(+)) and non-depressed (DEP(–)) subgroups. The 73 MCI/AD subjects with depressive symptoms were further subdivided according to their SSRI treatment. Subjects included in the analysis are highlighted in red.

sion scan with [^{68}Ge] or [^{137}Cs] rotating rod sources for PET-only scanners. Images were reconstructed using scanner-specific algorithms, and sent to the University of Michigan, where they were reviewed for artifacts and transmitted to the Laboratory of NeuroImaging (LONI) for storage.

Downloaded [^{18}F]-AV45-PET images in DICOM format had been preprocessed in four steps: 1) motion correction by co-registration of single 5-emin frames, 2) time frame averaging (50–70 min p.i.), 3) co-registration of longitudinal data to the baseline scan and reorientation in a standardized 160 × 160 × 96 matrix with 1.5 mm cubic voxels, and 4) smoothing with a scanner-specific filter function to an isotropic resolution of 8 mm, which is the ADNI standard designed to generate comparable images from different tomographs; this resolution represents the lowest resolution among scanners used in ADNI.

ADNI MRI acquisition and pre-processing

T1-weighted MRI scans had been acquired using Siemens, GE, or Philips MRI scanners according to a standard protocol [21] involving acquisitions of two 3D MPRAGE imaging sequences per subject. Of the two images acquired per subject and time-point, the ADNI quality assurance team selected the better image for preprocessing, based on the presence and severity of commonly-occurring image artifacts. MRI preprocessing involved: 1) application of a scanner-specific correction for gradient nonlinearity distortion (Gradwarp) [22]; 2) correction for image intensity non-uniformity (B1) [21]; 3) histogram peak sharpening algorithm for bias field correction (N3) [23]; 4) application of spatial scaling factors obtained by phantom measurements. For images acquired on Philips scanners, B1 correction was already implemented, and the gradient systems with this instrument tended to be linear [21]. More details on MRI image processing can be obtained from a previous investigation deriving from the ADNI cohort [24].

Image processing and analysis

The automated processing of the ADNI MRI and PET data, including quality control procedures, was performed in PNEURO (V 3.5, PMOD technologies, Basel, Switzerland) as previously described in detail [20]. In brief, T1-weighted MRI data were transferred into the Montreal Neurological Institute (MNI) standard space and subsequently segmented into gray matter, white matter, and cerebrospinal fluid (CSF). Segmented gray matter of each subject was further subdivided into 83 individual VOIs according to the brain atlas of Hammers [25]. Individual bilateral grey-matter VOIs of frontal (FRO), parietal (PAR), and temporal (TEMP) cortices, as well as the precuneal/posterior cingulate gyrus (PCC), and a composite (COMP) VOI, were used for the calculation of white matter-scaled individual

standard-uptake-value-ratios (SUVR) for each of the VOIs, which represent weighted sums of single VOIs. Results were obtained in PET native space after VOI-based partial volume effect correction (PVEC) using the method of Rousset [26] (Supplementary Figure 1), given that atrophy is especially apt to influence PET results in (cognitively-impaired) subjects with depressive symptoms [27]. Volumes (cm^3) of all grey matter VOIs were determined in MNI space. Subjects with failed PET processing were excluded prior to inclusion is this study (based on the experience with the dataset), and strong artifacts were masked [20, 27, 28].

Data analysis and statistics

PET SUVR values and grey matter volumes deriving from the VOIs (FRO, PAR, TEMP, PCC, and COMP), as well as cognition score (ADAS) were compared between the three different subject groups at baseline (BL) and calculated as absolute/percent change at the 2-year follow-up scan (absolute delta (Δ) / relative delta Δ%). Multivariate analysis of covariance (MANCOVA) with PET SUVR, grey matter volumes and cognition scores (ADAS) as dependent variables was performed with SPSS, version 23.0 (IBM, Chicago, IL). For BL analyses, subject age, ApoE-ε4 status, gender, and education level were used as covariates. For longitudinal analysis, BL amyloid burden (PET SUVR), and BL ADAS scores were included as additional covariates to minimize dispersion due to variable pathology burden at BL. Direct comparisons of main effects between the three groups after MANCOVA were performed using a Bonferroni correction per comparison. P values <0.05 were deemed significant after Bonferroni correction. The relationship between each subject's global amyloid burden (COMP) at BL and longitudinal changes in PET SUVR, grey matter volume, and ADAS scores was investigated by applying linear, logarithmic, and quadratic regression analyses as implemented in SPSS. In cases giving several statistically significant fits ($p < 0.05$), the best fitting model was identified by applying the Akaike information criterion (AIC) [29]. P values <0.1 were defined as a trend.

Necessary sample sizes for potential clinical trials of SSRI treatment versus placebo in cognitively affected patients were computed for DEP(+) patients. Longitudinal changes in ADAS and global grey matter volume were used as outcome parameter. Calculation was based on a t-test statistic with assumptions for a type I error $\alpha = 0.05$ and a power of 0.8. We note that this sample size calculation assumed a uniform mean effect on all subjects of a potential trial.

RESULTS

Demographics, cognition, and imaging values at baseline

There were no significant differences in age, gender, education, or ApoE ε4 status between the patient groups with and without depressive symptoms. Cognition as measured by ADAS was nearly equal between subgroups. The only significant group difference indicated less years of education in patients with SSRI-treatment compared to those with subsyndromal depression but without treatment (Table 1). 24/73 (33%) of the subjects were treated with an SSRI.

Regarding amyloid burden and grey matter volumes at BL, there were no significant differences between patient groups. All BL imaging values are provided in Supplementary Tables 1–2.

Longitudinal analysis of cognition

Comparing the DEP(+) and DEP(–) groups, we saw no significant differences in longitudinal changes in cognition (ADAS absolute-Δ: +1.0 / relative-Δ-%: +6.5% versus ADAS absolute-Δ: +1.3 / relative-Δ-%: +8.5%). Considering only those DEP(+) subjects receiving an SSRI treatment, we saw improvement in cognition, as indicated by a decrease in ADAS (absolute-Δ: –0.8 / relative-Δ-%: –5.0%), whereas the non-treated DEP(+) group deteriorated in cognition over the span of two years (absolute-Δ: +2.9 / relative-Δ-%: +18.6% ($p = 0.013$; MANCOVA, Bonferroni adjusted; Fig. 2). In the subgroup analysis of only Aβ(+) subjects, the same trend of longitudinal changes in ADAS was observed, although the difference between Aβ(+)/DEP(+) patients with SSRI treatment (absolute-Δ: +2.7 / relative-Δ-%: +15.6%) and those without (absolute-Δ: +5.1 / relative-Δ-%: +29.5%) was not significant ($p = 0.102$; MANCOVA, Bonferroni adjusted). Cognition followed longitudinally by MMSE gave similar results in this contrast; all cognition results are presented in Table 2.

Changing diagnoses were evaluated at follow-up when compared to BL: Of 225 MCI patients at BL, 29 (12.9%) converted to AD at the follow-up ($n = 17$ DEP(–); $n = 3$ DEP(+)/SSRI(+); $n = 9$ DEP(+)/SSRI(–)). 10 MCI patients (4.4%) were finally reverting to HC ($n = 6$ DEP(–); $n = 3$

Table 1
Demographics at Baseline, Aβ(+) subjects displayed separately

Study Group	Number (N)	Age ($y \pm SD$)	Gender (m / f)	Education ($y \pm SD$)	ADAS (mean ± SD)	ApoE (N ε4 (%))		
						0	1	2
All subjects								
DEP(+) total	73	71.8 ± 8.4	38 / 35	15.8 ± 2.7	15.2 ± 8.1	35 (48)	34 (47)	4 (5)
DEP(+)/SSRI(+)	24	71.6 ± 9.3	12 / 12	14.6 ± 2.9*	15.3 ± 7.2	13 (54)	11 (46)	0 (0)
DEP(+)/SSRI(–)	49	71.9 ± 8.0	26 / 23	16.4 ± 2.5	15.2 ± 8.6	22 (45)	23 (47)	4 (8)
DEP(–)	183	72.2 ± 8.0	100 / 83	16.3 ± 2.6	15.3 ± 8.1	98 (54)	66 (36)	19 (10)
Aβ(+) subjects								
DEP(+) total	42	75.3 ± 7.1	23 / 19	15.9 ± 3.0	18.5 ± 8.8	15 (36)	23 (55)	4 (9)
DEP(+)/SSRI(+)	15	77.2 ± 6.4	9 / 6	14.0 ± 3.3*	17.5 ± 7.6	7 (47)	8 (53)	0 (0)
DEP(+)/SSRI(–)	27	74.3 ± 7.3	14 / 13	16.9 ± 2.2	19.1 ± 9.5	8 (30)	15 (56)	4 (15)
DEP(–)	96	74.4 ± 7.4	58 / 38	15.8 ± 2.8	18.6 ± 8.9	38 (40)	41 (43)	17 (18)

Significant differences between DEP(+)/SSRI(+) and DEP(+)/SSRI(–) are indicated by $^{*}p < 0.05$. No significant differences were observed between DEP(+) total and DEP(–). MANCOVA with testing of main effects and Bonferroni adjustment was used for intergroup comparison.

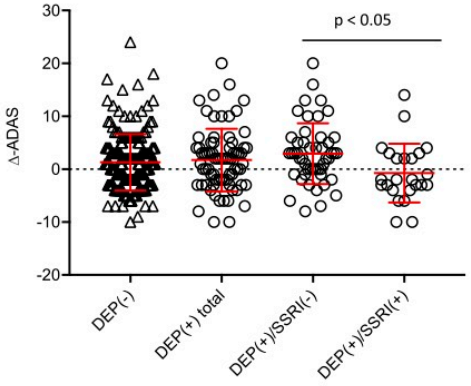

Fig. 2. Longitudinal course of ADAS for the two main groups of DEP(+) total and DEP(–) as well as for DEP(+)/SSRI(+) and DEP(+)/SSRI(–) subgroups. MANCOVA with testing of main effects and Bonferroni adjustment was used for intergroup comparison.

DEP(+)/SSRI(+); $n = 1$ DEP(+)/SSRI(–)). From 31 AD-cases at BL, one (3.2%) was classified as MCI at the follow-up scan (DEP(+)/SSRI(+)), whereas 30 (96.8%) remained AD.

Longitudinal analysis of amyloid burden and grey matter volume

In the next step, we investigated changes in amyloid burden and grey matter volume during the 2-year interval in relation to depressive symptom and SSRI-treatment status.

Longitudinal Aβ deposition rates

Comparing the entire groups of depressed and non-depressed individuals, we saw only a small difference in the mean longitudinal increase of Aβ burden (Δ%-COMP-SUVR: +5.0% versus +5.6% $p = 0.568$; MANCOVA, Bonferroni adjusted). In the analysis of subsyndromal depressed patients with and without SSRI treatment, there was only a slight trend towards lower amyloid deposition rates in SSRI(+) patients, most notably in the frontal cortex (Δ%-FRO-SUVR: +5.0% versus +6.1%; $p = 0.635$; MANCOVA, Bonferroni adjusted; Supplementary Table 3A); results were similar in the subanalysis of Aβ(+) subjects. Here the frontal lobe likewise showed the highest difference of amyloid deposition rate (Δ%-FRO-SUVR) as a function of SSRI

Table 2
Baseline scores, follow-up scores and longitudinal changes (Δ%) of cognitive testing (ADAS, MMSE) are provided. All follow-up values and longitudinal changes are adjusted for the baseline ADAS

Study Group	ADAS at Baseline		ADAS at follow-up/ ADAS Δ%-BL/FU		MMSE at Baseline		MMSE at follow-up/ MMSE Δ%-BL/FU	
	All	Aβ(+)	All	Aβ(+)	All	Aβ(+)	All	Aβ(+)
DEP(+) total	15.2	18.0	16.3/+6.5%	22.0/+16.6%	27.6	26.5	26.7/–3.3%	25.3/–4.5%
DEP(+)/SSRI(+)	15.3	17.5	14.5/–5.0%*	20.6/+9.3%	27.8	27.5	27.7/–0.4%**	26.5/–3.6%*
DEP(+)/SSRI(–)	15.2	19.1	18.1/+18.6%*	23.4/+24.2%	27.3	26.5	25.8/–5.5%**	24.0/–9.4%*
DEP(–)	15.3	18.6	16.6/+8.5%	21.4/+13.6%	27.5	27.0	26.5/–3.6%	24.8/–2.2%

Significant differences between DEP(+)/SSRI(–) and DEP(–)/SSRI(–) are indicated by $^{*}p < 0.05$, $^{**}p < 0.005$. MANCOVA with testing of main effects and Bonferroni adjustment was used for statistical intergroup comparison. No significant differences were observed between DEP(+) total and DEP(–).

treatment (DEP(+)/SSRI(+) versus DEP(+)/SSRI(–): +3.8% versus +7.0%; $p = 0.261$; MANCOVA, Bonferroni adjusted; Supplementary Table 3B). For the exact values, we refer the reader to the Supplementary Table 3A and B.

Longitudinal grey matter volume measurements

Subsyndromal depressed subjects and the non-depressed group revealed similar decreases of total grey matter volume to 2-year follow-up (Δ%-VOL: 1.8% versus 1.7%; p = n.s.; MANCOVA, Bonferroni adjusted); subregion analysis gave similar results. Subgroup analysis showed a loss of only 0.9% of total grey matter volume in SSRI(+) patients, whereas SSRI(–) subsyndromal depressed lost 2.7% ($p = 0.031$; MANCOVA, Bonferroni adjusted). To subregion analysis, the greatest volume loss was in frontal and temporal cortices (Δ%-VOL FRO: –0.8% versus 2.7%; $p = 0.042$; MANCOVA, Bonferroni adjusted / Δ%-VOL TEMP $p = 0.016$; MANCOVA, Bonferroni adjusted) (Table 3A).

To find more specific region-related differences we measured volumes in 64 cortical and subcortical segmented VOIs of Hammer's atlas, of which 14 regions showed significant difference between SSRI(+) and SSRI(–) subsyndromally depressed subjects (Supplementary Table 4).

Subanalysis in Aβ(+) patients indicated similar results, with a higher mean atrophy rate in those patients with subsyndromal depression. In particular, the SSRI-treated DEP(+) group of Aβ(+) patients had significantly less progression of atrophy in the temporal lobe (Δ%-VOL: –1.1% versus –3.9%; $p = 0.009$; MANCOVA, Bonferroni adjusted), the PCC (Δ%-VOL: –1.2% versus –4.4%; $p = 0.030$; MANCOVA, Bonferroni adjusted), and also in the total grey matter volume (Δ%-VOL: –1.4% versus –3.8%; $p = 0.040$; MANCOVA, Bonferroni adjusted) when compared to untreated Aβ(+)/DEP(+) patients (Table 3B). Two individual examples of grey matter atrophy of a pair of Aβ(+) patients with and without SSRI treatment are shown in Fig. 3.

Relationship between baseline Aβ-PET and longitudinal read-outs

Establishing a linkage between BL amyloid level and the further progression of cognition decline could help to predict outcome in single patients. Therefore, we conducted regression analyses for the three different cohorts. In this analysis, BL Aβ levels positively correlated with longitudinal cognitive decline in all study groups (at trend for DEP(+)/SSRI(+)); quadratic functions gave the best fit in all study groups (Fig. 4). Visually, the shape of the function of Δ-ADAS with higher Aβ BL levels had a slightly more pronounced increase in the group of DEP(+)/SSRI(–) subjects when compared to the DEP(–) subjects. This could indicate that patients with subsyndromal depression and high initial amyloid load decline faster compared to DEP(–) patients, as we have likewise seen in our previous investigation [10]. The degree of rescue of declining cognitive performance by SSRI medication in relation to individual BL Aβ levels was characterized by a global shift to lower Δ-ADAS when comparing DEP(+)/SSRI(+) with DEP(+)/SSRI(–), such that the function of the relationship DEP(+)/SSRI(+) clearly ranged below that of the DEP(–) group. Quantitatively, individual SSRI-treated DEP(+) patients had 5.0 ± 2.6% (range: 2.3 – 11.3%) less increase in Δ-ADAS over two years when compared to DEP(+)/SSRI(–).

There were no significant associations between BL Aβ-PET and longitudinal change of the amyloid burden or changes in grey matter atrophy, probably due to the clinical heterogeneity expected in such a cohort of subjects.

Necessary sample sizes for prospective clinical trials

Calculation of required sample sizes for prospective clinical trial of SSRI versus placebo gave $n = 76$ ($n = 38$ for each group of DEP(+)/SSRI(+) and DEP(+)/SSRI(–) patients) for absolute ADAS as the

Table 3A
2-year follow-up of grey matter volumes; significant differences between DEP(+)/SSRI(+) and DEP(+)/SSRI(–) are indicated by $^{*}p < 0.05$ / $^{**}p < 0.001$

Study Group	Δ%-VOL FRO	Δ%-VOL PAR	Δ%-VOL TEMP	Δ%-VOL PCC	Δ%-VOL COMP
DEP(+) total	–1.8% (±3.6%)	–2.0% (±3.8%)	–1.7% (±3.0%)	–2.1% (±4.2%)	–1.8% (±3.2%)
DEP(+)/SSRI(+)	–0.8%* (±4.0%)	–1.3% (±3.8%)	–0.9%* (±3.0%)	–1.2% (±3.3%)	–0.9%* (±3.4%)
DEP(+)/SSRI(–)	–2.7%* (±3.2%)	–2.7% (±3.8%)	–2.6%* (±3.0%)	–3.0% (±4.5%)	–2.7%* (±2.9%)
DEP(–)	–1.6% (±3.7%)	–1.7% (±4.0%)	–1.7% (±3.0%)	–1.3% (±3.6%)	–1.7% (±3.2%)

No significant differences were observed between DEP(+) total and DEP(–). MANCOVA with testing of main effects and Bonferroni adjustment was used for statistical intergroup comparison.

Table 3B
2-year follow-up of grey matter volumes in Aβ(+) subjects; significant differences between DEP(+)/SSRI(+) and DEP(+)/SSRI(–) are indicated by $^{*}p < 0.05$ / $^{**}p < 0.001$

Study Group	Δ%-VOL FRO	Δ%-VOL PAR	Δ%-VOL TEMP	Δ%-VOL PCC	Δ%-VOL COMP
DEP(+) total	–2.6% (±3.9%)	–2.9% (±4.4%)	–2.5% (±3.2%)	–2.8% (±5.0%)	–2.6% (±3.4%)
DEP(+)/SSRI(+)	–1.3% (±4.4%)	–2.2% (±4.1%)	–1.1%** (±3.1%)	–1.2%* (±3.0%)	–1.4%* (±3.7%)
DEP(+)/SSRI(–)	–3.8% (±3.3%)	–3.6% (±4.5%)	–3.9%** (±3.0%)	–4.4%* (±5.6%)	–3.8%* (±3.0%)
DEP(–)	–1.8% (±3.9%)	–2.0% (±4.4%)	–2.1% (±3.2%)	–1.4% (±4.0%)	–2.0% (±3.5%)

No significant differences were observed between DEP(+) total and DEP(–). MANCOVA with testing of main effects and Bonferroni adjustment was used for statistical intergroup comparison.

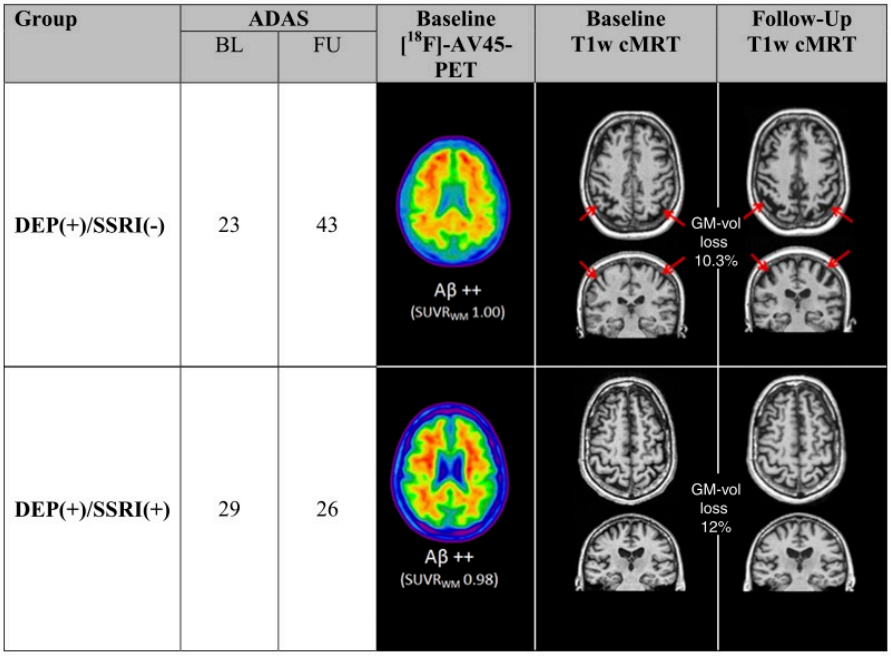

Fig. 3. Two DEP(+), Aβ(+) subjects with similar baseline are illustrated, both indicating elevated ADAS at baseline with comparable amyloid load (cutoff of Aβ positivity: 0.77). Progression of grey matter atrophy was pronounced in the SSRI(–) case (red arrows). Two representative examples at the opposite extreme of grey matter atrophy progression depict the range of results.

endpoint and $n = 90$ ($n = 45$ each) for relative ADAS. Corresponding sample sizes in the Aβ(+) subgroup were $n = 60$ ($n = 30$ each) for absolute ADAS and $n = 124$ ($n = 62$ each) for relative ADAS, with larger sample sizes reflecting the higher variance of cognition changes in this subgroup.

Longitudinal measures of atrophy required a sample size of $n = 78$ ($n = 39$ each) for the global grey matter volume and $n = 80$ ($n = 40$ each) for the temporal grey matter volume in the same contrast of DEP(+)/SSRI(+) versus DEP(+)/SSRI(–) patients. Corresponding sample sizes in the Aβ(+) subgroup were $n = 52$ ($n = 26$ each) for the global grey matter volume and $n = 32$ ($n = 16$ each) for the temporal grey matter volume.

DISCUSSION

We present the results of a 2-year longitudinal follow-up analysis aiming to test for effects of SSRI treatment on cognitive performance, amyloid burden and grey matter volume in cognitively affected subjects with coexisting subsyndromal depression. Multivariate analyses revealed that subjects with depressive symptoms were characterized by faster cognitive decline if not receiving SSRI treatment.

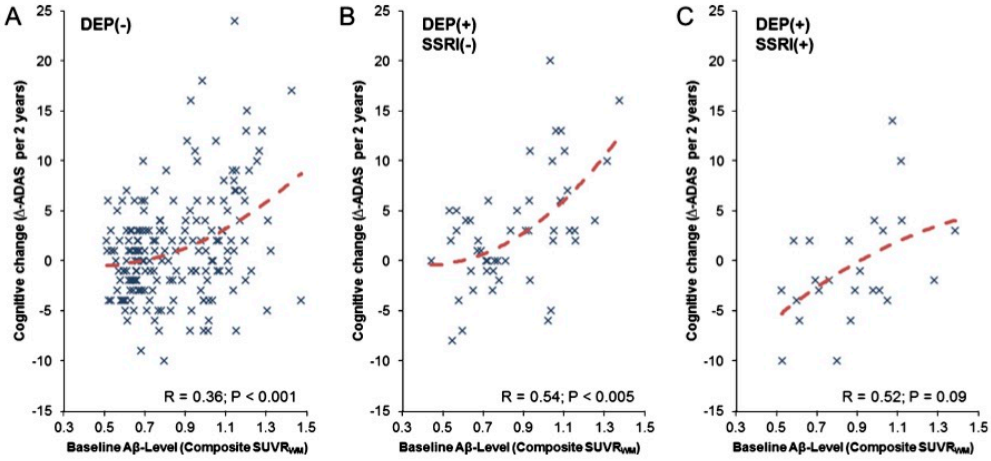

Fig. 4. Relationship between the baseline amyloid-β (Aβ) level and cognitive change (Δ-ADAS) during two y for all three study groups (A-C). Dashed red lines represent the non-linear function between both parameters, which gave a quadratic fit as the best model for all subgroups.

Additionally, structural imaging indicated a faster progression of grey matter atrophy especially in the frontal lobe of subjects with depressive symptoms and lacking SSRI treatment. The attenuation of amyloid progression by SSRI treatment reported in a preclinical setting was not observed in the present clinical cohort. Moreover, the SSRI treatment rescued cognitive decline irrespective of the individual cerebral amyloid burden at BL. In summary, SSRI treatment imparted a beneficial effect on longitudinal cognitive performance in subjects with dementia symptoms and subsyndromal depression, accompanied by rescue of grey matter atrophy, but without significant effects on amyloid burden.

Cognition

In this investigation, we used *in vivo* biomarkers derived from PET and MRI imaging to characterize progression of symptoms in groups of patients with highly heterogeneous presentation of dementia and depression. By correction for differences in individual amyloid burden at BL, in addition to consideration of more standard covariates, we were in an earlier study able to account for the individual progression of amyloid burden to follow-up [30]. In this subsequent analysis of cognitive performance, there was little difference in BL ADAS and MMSE scores between the DEP(+) and DEP(–) groups at BL and in the longitudinal run. However, the stratification of DEP(+) in SSRI treatment/non-treatment subgroups revealed a significantly better outcome with respect to preservation of cognition in those patients receiving SSRI treatment during the follow-up period of two years. Others have found significantly improved MMSE scores after 3 months of SSRI treatment in AD patients [31], while a recent review including 10 randomized controlled trails and 3 meta-analyses on antidepressants in depressed AD patients reported inconsistent results, and suggested treatment by non-pharmacologic approaches and watchful waiting if depressive symptoms are not severe [32]. We note that only 24 of 73 (32.9%) MCI and AD subjects reporting depressive symptoms in NPI-Q were treated with antidepressant medication in our current ADNI sample. Others have likewise found an under-treatment, with only 45% of AD subjects with depressive symptoms receiving SSRIs in a 108-month follow up study [33]. As a Geriatric Depression Score (GDS) of higher than 5 is an exclusion criterion in ADNI, it has to be considered that the depressive symptoms of our study group were relatively low (GDS positive (3/73), mean GDS: 2.4), which possibly accounts for the low rate of SSRI treatment. Under consideration of the small sample size of subjects with depressive symptoms, present results suggest that SSRI treatment may be indicated even for minor depressive symptoms in patients with cognitive impairment, as sparing from cognitive decline was clearly evident to the present 2-year follow-up.

As Aβ-negative as well as -positive cases seem to benefit from the SSRI treatment, it must be

considered whether the treatment affects the AD-specific pathology or the common course of dementia diseases. In this regard, MCI subjects show a wide range of pathological findings in autopsy, which is still subject to further studies [34]. From our data, the underlying mechanism of the SSRI-treatment may not specifically concern the AD-pathology but more likely a final common pathway of neurodegeneration. Speculatively, this could be a neuroinflammatory process, which is evidently common to nearly all neurodegenerative diseases [35], and is seemingly ameliorated by SSRI treatment [36, 37].

Amyloid burden

Based on the preclinical study of Sheline and colleagues in AD model mice [17], we predicted a lower progression rate of amyloidosis with SSRI-treatment during 2-year follow-up, as SSRIs significantly delayed amyloidogenesis in the mouse model. The same research group also found lower amyloid burden to [^{11}C]-PiB-PET in cognitively healthy subjects with a history of SSRI intake when compared to SSRI-naive subjects, and also reported a negative correlation between amyloid burden and duration of previous SSRI intake [16]. Our hypothesis was not supported by the present longitudinal *in vivo* assessment of amyloid burden in a mixed group of MCI and AD patients examined with [^{18}F]-AV45-PET. In this regard, our retrospective study design entails certain limitations, in that we were unable to assess the initiation date of the SSRI treatment, nor was the dose recorded. Thus, it may be that the main effect of SSRI treatment on amyloidosis in the individual subject had already transpired prior to the 2-year PET study period in this investigation, although we note that our BL assessments of amyloid burden do not support this speculation (Supplementary Table 1A, B). Furthermore, our subjects already had progressed towards cognitive decline at entry in the study, and many had rather high amyloid burden in the brain. In general, pharmacological effects on ongoing amyloid deposition would likely be more evident when initiated an early stage of amyloidosis [38].

Nonetheless, we contend that amyloid PET constituted an important methodological feature in this study as it enabled us to take into consideration the individual amyloidosis at BL, which was of proven benefit in an earlier preclinical investigation [38]. This correction for individual magnitude of amyloid pathology at BL increased the sensitivity for discerning changes to follow-up in a heterogenous study population. We feel that molecular imaging investigations in heterogeneous conditions like dementia and depression highly benefit from such BL scaling, as high amyloid levels at BL bring *per se* a tremendous risk for rapid cognitive decline [39]. Indeed, we find a significant positive relationship between BL amyloid burden and change in ADAS over two years in all subgroups of our study, albeit at trend level for the DEP(+)/SSRI(+) subgroup (Fig. 4). The benefit of SSRI treatment on rescue from longitudinal decline in cognition seems to occur irrespectively of the initial amyloid load, although the small sample size precluded strong claims to this effect.

Brain atrophy

Analysis of brain atrophy suggested higher grey matter volume loss in subsyndromal depressed subjects when compared to those without depressive symptoms, a difference that was most pronounced in the subanalysis of amyloid-positive subjects. Similar findings were reported in a recent study, wherein depressive symptoms in AD patients were associated with cortical thinning, especially in temporal and parietal regions [40]. Another study revealed that depressive symptoms in MCI subjects were linked with greater atrophy in AD-affected brain regions [41]. The frontal lobe is also reported to show grey matter atrophy in non-demented patients with major depressive disorder [42]. Therefore, there is evidently a connection between depressive symptoms and brain atrophy in patients with cognitive impairment. Importantly, we do not find differences in atrophy rates between patients with and without depressive symptoms when SSRI treatment is not considered, perhaps due to a balancing of opposing effects in treated and untreated patients. However, our analysis of SSRI treatment in subsyndromal depressed subjects indicated a clear rescue of atrophy rate in the 2-year follow up, especially in frontal and temporal regions. The most significantly spared VOIs included regions implicated in AD (temporal gyri) but were predominantly found in mood-related brain networks (e.g., orbitofrontal and anterior cingulate gyri) [43, 44]. The SSRI treatment slowed brain atrophy, probably constituting the macroscopic or anatomic correlate to the positive effects on cognitive performance. It should be considered that volumetric and cognitive changes did not correlate on the individual level, probably due to the inherent heterogeneity in such samples. However, the present structural imaging-related findings confirm that SSRI treatment brings

not only a clinical improvement of subsyndromal depressive symptoms, but likewise has a beneficial structural correlate during the 2-year follow-up.

The finding of lower progression of atrophy in the SSRI treatment group was similar when investigating Aβ(+) subjects only. Therefore, we see not clear linkage between underlying amyloid pathology and the positive effect of SSRI treatment. The underlying mechanism of this beneficial effect on the grey matter volume remains to be elucidated, but we can assume that the ongoing neurodegeneration in DEP(+) patients might be modulated by SSRI treatment independently from the degree of amyloid burden.

Limitations

Subsyndromal depressed patients were stratified by NPI-Q, as there was no clinical diagnosis of depression and no gold standard structured interview data available. Hence, the low sensitivity of this single item must be considered as a limitation of our study. We considered using the geriatric depression scale, but this was rejected since any GDS >5 was defined as an exclusion criterion of ADNI; as this criterion might have led to more selection bias, we elected to the NPI-Q score. Furthermore, the documentation of SSRI-treatment begins only at the time of the BL PET scan, such that we cannot ascertain the duration of SSRI treatment, which may have some bearing on the amyloid load, cognition, and brain atrophy seen in the ADNI inclusion period. Indeed, depressive symptoms in the time before ADNI inclusion are unknown. Thus, our findings might be confounded by subsuming subjects with and without history of SSRI treatment when they had no depressive symptoms at entry into the study. Our patient group could potentially include patients with earlier depressive symptoms that resolved upon treatment. However, due to the broad medical indications for SSRI, we considered the present approach as preferable, regarding potential bias deriving from patients treated with SSRI for reasons other than depressive symptoms. Another limitation consists of the different and particularly unknown SSRI dosages, such that known SSRI dosage effects cannot be considered in our study [45]. Furthermore, the effectiveness of SSRI treatment for depressive symptoms shows great inter-individual variation [46], which might be a limitation in the comparison of treated subjects with individual response to the treatment. However, we emphasize that sufficiently powered molecular imaging studies are poised to play an important future role in compensation for such heterogeneous responses. A further limitation due to the retrospective design lies in the relatively small number ($n = 24$) of SSRI-treated subsyndromal depressed patients. However, our study entails relatively large comparison groups ($n = 49/n = 183$), and the benefits of normalization to BL covariates strengthens the conclusions to be drawn in a very specific subgroup. As more than 90% of our subjects had BL and follow-up scans on the same scanner, scanner-specific differences could conceivable interact with actual biological changes. Finally, we used pre-processed data from the ADNI set, and did not perform additional longitudinal processing of MRI scans as performed by other investigations [47]. Thus, we cannot fully exclude a bias deriving from scanner-related measurement errors between BL and follow-up MRI scans, but larger errors should have been avoided by our highly sophisticated quality control [28]. Correction for multiple comparisons was applied to adjust for more than two subgroups but not for the different outcome parameter of the study, thus the results of this exploratory study should be interpreted carefully.

Conclusions

Our results indicate that cognitively impaired subjects with MCI or AD in conjunction with depressive symptoms benefit from SSRI treatment regarding rescue from longitudinal decline in cognitive performance. As a structural correlate of the clinical cognitive benefits, lower grey matter atrophy rates were observed during the 2-year follow-up in these patients. Contrary to expectation, we saw only small trends towards a beneficial effect SSRI treatment on amyloid deposition rates. Given the low proportion of SSRI-treated patients in this sample, we contend that more attention should be placed on depressive symptoms in the field of AD research, even when these symptoms are subsyndromal. Finally, our *in vivo* assessment of amyloid burden by PET at BL allows individual scaling/normalization of a rather heterogeneous sample, an approach with considerable potential for improving the sensitivity of clinical antidepressant trials in AD.

ACKNOWLEDGMENTS

Language editing was provided by Inglewood Biomedical Editing. This paper originated from the doctoral thesis of Julia Sauerbeck.

Data collection and sharing for this project was funded by the Alzheimer's Disease Neuroimaging Initiative (ADNI) (National Institutes of Health Grant U01 AG024904) and DOD ADNI (Department of Defense award number W81XWH-12-2-0012). ADNI is funded by the National Institute on Aging, the National Institute of Biomedical Imaging and Bioengineering, and through generous contributions from the following: AbbVie, Alzheimer's Association; Alzheimer's Drug Discovery Foundation; Araclon Biotech; BioClinica, Inc.; Biogen; Bristol-Myers Squibb Company; CereSpir, Inc.; Cogstate; Eisai Inc.; Elan Pharmaceuticals, Inc.; Eli Lilly and Company; EuroImmun; F. Hoffmann-La Roche Ltd and its affiliated company Genentech, Inc.; Fujirebio; GE Healthcare; IXICO Ltd.; Janssen Alzheimer Immunotherapy Research & Development, LLC.; Johnson & Johnson Pharmaceutical Research & Development LLC.; Lumosity; Lundbeck; Merck & Co., Inc.; Meso Scale Diagnostics, LLC.; NeuroRx Research; Neurotrack Technologies; Novartis Pharmaceuticals Corporation; Pfizer Inc.; Piramal Imaging; Servier; Takeda Pharmaceutical Company; and Transition Therapeutics. The Canadian Institutes of Health Research is providing funds to support ADNI clinical sites in Canada. Private sector contributions are facilitated by the Foundation for the National Institutes of Health (http://www.fnih.org). The grantee organization is the Northern California Institute for Research and Education, and the study is coordinated by the Alzheimer's Therapeutic Research Institute at the University of Southern California. ADNI data are disseminated by the Laboratory for Neuro Imaging at the University of Southern California.

Authors' disclosures available online (https://www.j-alz.com/manuscript-disclosures/17-0387r3).

SUPPLEMENTARY MATERIAL

The supplementary material is available in the electronic version of this article: http://dx.doi.org/10.3233/JAD-170387.

REFERENCES

[1] Ownby RL, Crocco E, Acevedo A, John V, Loewenstein D (2006) Depression and risk for Alzheimer disease: Systematic review, meta-analysis, and metaregression analysis. *Arch Gen Psychiatry* **63**, 530-538.

[2] Steenland K, Karnes C, Seals R, Carnevale C, Hermida A, Levey A (2012) Late-life depression as a risk factor for mild cognitive impairment or Alzheimer's disease in 30 US Alzheimer's disease centers. *J Alzheimers Dis* **31**, 265-275.

[3] Olin JT, Katz IR, Meyers BS, Schneider LS, Lebowitz BD (2002) Provisional diagnostic criteria for depression of Alzheimer disease: Rationale and background. *Am J Geriatr Psychiatry* **10**, 129-141.

[4] Mackin RS, Insel P, Tosun D, Mueller SG, Schuff N, Truran-Sacrey D, Raptentsetsang ST, Lee JY, Jack CR Jr, Aisen PS, Petersen RC, Weiner MW; Alzheimer's Disease Neuroimaging Initiative (2013) The effect of subsyndromal symptoms of depression and white matter lesions on disability for individuals with mild cognitive impairment. *Am J Geriatr Psychiatry* **21**, 906-914.

[5] Mosconi L, Berti V, Glodzik L, Pupi A, De Santi S, de Leon MJ (2010) Pre-clinical detection of Alzheimer's disease using FDG-PET, with or without amyloid imaging. *J Alzheimers Dis* **20**, 843-854.

[6] Adlard PA, Tran BA, Finkelstein DI, Desmond PM, Johnston LA, Bush AI, Egan GF (2014) A review of β-amyloid neuroimaging in Alzheimer's disease. *Front Neurosci* **8**, 327.

[7] Ossenkoppele R, Jansen WJ, Rabinovici GD, Knol DL, van der Flier WM, van Berckel BN, Scheltens P, Visser PJ; Amyloid PET Study Group, Verfaillie SC, Zwan MD, Adriaanse SM, Lammertsma AA, Barkhof F, Jagust WJ, Miller BL, Rosen HJ, Landau SM, Villemagne VL, Rowe CC, Lee DY, Na DL, Seo SW, Sarazin M, Roe CM, Sabri O, Barthel H, Koglin N, Hodges J, Leyton CE, Vandenberghe R, van Laere K, Drzezga A, Forster S, Grimmer T, Sánchez-Juan P, Carril JM, Mok V, Camus V, Klunk WE, Cohen AD, Meyer PT, Hellwig S, Newberg A, Frederiksen KS, Fleisher AS, Mintun MA, Wolk DA, Nordberg A, Rinne JO, Chételat G, Lleo A, Blesa R, Fortea J, Madsen K, Rodrigue KM, Brooks DJ (2015) Prevalence of amyloid PET positivity in dementia syndromes: A meta-analysis. *JAMA* **313**, 1939-1949.

[8] Wu KY, Hsiao IT, Chen CS, Chen CH, Hsieh CJ, Wai YY, Chang CJ, Tseng HJ, Yen TC, Liu CY, Lin KJ (2013) Increased brain amyloid deposition in patients with a lifetime history of major depression: Evidenced on 18F-florbetapir (AV-45/Amyvid) positron emission tomography. *Eur J Nucl Med Mol Imaging* **41**, 714-722.

[9] Wu KY, Liu CY, Chen CS, Chen CH, Hsiao IT, Hsieh CJ, Lee CP, Yen TC, Lin KJ (2016) Beta-amyloid deposition and cognitive function in patients with major depressive disorder with different subtypes of mild cognitive impairment: (18)F-florbetapir (AV-45/Amyvid) PET study. *Eur J Nucl Med Mol Imaging* **43**, 1067-1076.

[10] Brendel M, Pogarell O, Xiong G, Delker A, Bartenstein P, Rominger A; Alzheimer's Disease Neuroimaging Initiative (2015) Depressive symptoms accelerate cognitive decline in amyloid-positive MCI patients. *Eur J Nucl Med Mol Imaging* **42**, 716-724.

[11] Harrington KD, Gould E, Lim YY, Ames D, Pietrzak RH, Rembach A, Rainey-Smith S, Martins RN, Salvado O, Villemagne VL, Rowe CC, Masters CL, Maruff P; AIBL Research Group (2017) Amyloid burden and incident depressive symptoms in cognitively normal older adults. *Int J Geriatr Psychiatry* **32**, 453-463.

[12] Chung JK, Plitman E, Nakajima S, Chakravarty MM, Caravaggio F, Gerretsen P, Iwata Y, Graff-Guerrero A; Alzheimer's Disease Neuroimaging Initiative (2016) Cortical amyloid β deposition and current depressive symptoms in Alzheimer disease and mild cognitive impairment. *J Geriatr Psychiatry Neurol* **29**, 149-159.

[13] Jones HE, Joshi A, Shenkin S, Mead GE (2016) The effect of treatment with selective serotonin reuptake inhibitors in comparison to placebo in the progression of dementia: A systematic review and meta-analysis. *Age Ageing* **45**, 448-456.

[14] Namekawa Y, Baba H, Maeshima H, Nakano Y, Satomura E, Takebayashi N, Nomoto H, Suzuki T, Arai H (2013) Heterogeneity of elderly depression: Increased risk of Alzheimer's disease and Aβ protein metabolism. *Prog Neuropsychopharmacol Biol Psychiatry* **43**, 203-208.

[15] Harrington KD, Lim YY, Gould E, Maruff P (2015) Amyloid-beta and depression in healthy older adults: A systematic review. *Aust N Z J Psychiatry* **49**, 36-46.

[16] Cirrito JR, Disabato BM, Restivo JL, Verges DK, Goebel WD, Sathyan A, Hayreh D, D'Angelo G, Benzinger T, Yoon H, Kim J, Morris JC, Mintun MA, Sheline YI (2011) Serotonin signaling is associated with lower amyloid-β levels and plaques in transgenic mice and humans. *Proc Natl Acad Sci U S A* **108**, 14968-14973.

[17] Sheline YI, West T, Yarasheski K, Swarm R, Jasielec MS, Fisher JR, Ficker WD, Yan P, Xiong C, Frederiksen C, Grzelak MV, Chott R, Bateman RJ, Morris JC, Mintun MA, Lee JM, Cirrito JR (2014) An antidepressant decreases CSF Aβ production in healthy individuals and in transgenic AD mice. *Sci Transl Med* **6**, 236re234.

[18] Kaufer DI, Cummings JL, Ketchel P, Smith V, MacMillan A, Shelley T, Lopez OL, DeKosky ST (2000) Validation of the NPI-Q, a brief clinical form of the Neuropsychiatric Inventory. *J Neuropsychiatry Clin Neurosci* **12**, 233-239.

[19] Jack CR Jr, Bennett DA, Blennow K, Carrillo MC, Feldman HH, Frisoni GB, Hampel H, Jagust WJ, Johnson KA, Knopman DS, Petersen RC, Scheltens P, Sperling RA, Dubois B (2016) A/T/N: An unbiased descriptive classification scheme for Alzheimer disease biomarkers. *Neurology* **87**, 539-547.

[20] Brendel M, Högenauer M, Delker A, Sauerbeck J, Bartenstein P, Seibyl J, Rominger A; Alzheimer's Disease Neuroimaging Initiative (2015) Improved longitudinal [(18)F]-AV45 amyloid PET by white matter reference and VOI-based partial volume effect correction. *Neuroimage* **108**, 450-459.

[21] Jack CR Jr, Bernstein MA, Fox NC, Thompson P, Alexander G, Harvey D, Borowski B, Britson PJ, L Whitwell J, Ward C, Dale AM, Felmlee JP, Gunter JL, Hill DL, Killiany R, Schuff N, Fox-Bosetti S, Lin C, Studholme C, DeCarli CS, Krueger G, Ward HA, Metzger GJ, Scott KT, Mallozzi R, Blezek D, Levy J, Debbins JP, Fleisher AS, Albert M, Green R, Bartzokis G, Glover G, Mugler J, Weiner MW (2008) The Alzheimer's Disease Neuroimaging Initiative (ADNI): MRI methods. *J Magn Reson Imaging* **27**, 685-691.

[22] Jovicich J, Czanner S, Greve D, Haley E, van der Kouwe A, Gollub R, Kennedy D, Schmitt F, Brown G, Macfall J, Fischl B, Dale A (2006) Reliability in multi-site structural MRI studies: Effects of gradient non-linearity correction on phantom and human data. *Neuroimage* **30**, 436-443.

[23] Sled JG, Zijdenbos AP, Evans AC (1998) A nonparametric method for automatic correction of intensity nonuniformity in MRI data. *IEEE Trans Med Imaging* **17**, 87-97.

[24] Weiner MW, Veitch DP, Aisen PS, Beckett LA, Cairns NJ, Cedarbaum J, Green RC, Harvey D, Jack CR, Jagust W, Luthman J, Morris JC, Petersen RC, Saykin AJ, Shaw L, Shen L, Schwarz A, Toga AW, Trojanowski JQ; Alzheimer's Disease Neuroimaging Initiative (2015) 2014 Update of the Alzheimer's Disease Neuroimaging Initiative: A review of papers published since its inception. *Alzheimers Dement* **11**, e1-e120.

[25] Hammers A, Allom R, Koepp MJ, Free SL, Myers R, Lemieux L, Mitchell TN, Brooks DJ, Duncan JS (2003) Three-dimensional maximum probability atlas of the human brain, with particular reference to the temporal lobe. *Hum Brain Mapp* **19**, 224-247.

[26] Rousset OG, Ma Y, Evans AC (1998) Correction for partial volume effects in PET: Principle and validation. *J Nucl Med* **39**, 904-911.

[27] Brendel M, Reinisch V, Kalinowski E, Levin J, Delker A, Därr S, Pogarell O, Förster S, Bartenstein P, Rominger A; Alzheimer's Disease Neuroimaging Initiative (2016) Hypometabolism in brain of cognitively normal patients with depressive symptoms is accompanied by atrophy-related partial volume effects. *Curr Alzheimer Res* **13**, 475-486.

[28] Högenauer M, Brendel M, Delker A, Därr S, Weiss M, Bartenstein P, Rominger A; Alzheimer's Disease Neuroimaging Initiative (2016) Impact of MRI-based segmentation artifacts on amyloid- and FDG-PET quantitation. *Curr Alzheimer Res* **13**, 597-607.

[29] Akaike H (1973) Information theory and an extension of the maximum likelihood principle. In: Petrov BN, Csaki F, editors. *Second International Symposium on Information Theory*; Budapest Akademiai Kiado, pp. 267-281.

[30] Jack CR Jr, Holtzman DM (2013) Biomarker modeling of Alzheimer's disease. *Neuron* **80**, 1347-1358.

[31] Mokhber N, Abdollahian E, Soltanifar A, Samadi R, Saghebi A, Haghighi MB, Azarpazhooh A (2014) Comparison of sertraline, venlafaxine and desipramine effects on depression, cognition and the daily living activities in Alzheimer patients. *Pharmacopsychiatry* **47**, 131-140.

[32] Leong C (2014) Antidepressants for depression in patients with dementia: A review of the literature. *Consult Pharm* **29**, 254-263.

[33] Barry LC, Abou JJ, Simen AA, Gill TM (2012) Undertreatment of depression in older persons. *J Affect Disord* **136**, 789-796.

[34] Mufson EJ, Binder L, Counts SE, DeKosky ST, de Toledo-Morrell L, Ginsberg SD, Ikonomovic MD, Perez SE, Scheff SW (2012) Mild cognitive impairment: Pathology and mechanisms. *Acta Neuropathol* **123**, 13-30.

[35] Stefaniak J, O'Brien J (2016) Imaging of neuroinflammation in dementia: A review. *J Neurol Neurosurg Psychiatry* **87**, 21-28.

[36] Zhang F, Zhou H, Wilson BC, Shi JS, Hong JS, Gao HM (2012) Fluoxetine protects neurons against microglial activation-mediated neurotoxicity. *Parkinsonism Relat Disord* **18 Suppl 1**, S213-S217.

[37] Liu RP, Zou M, Wang JY, Zhu JJ, Lai JM, Zhou LL, Chen SF, Zhang X, Zhu JH (2014) Paroxetine ameliorates lipopolysaccharide-induced microglia activation via differential regulation of MAPK signaling. *J Neuroinflammation* **11**, 47.

[38] Brendel M, Jaworska A, Herms J, Trambauer J, Rotzer C, Gildehaus FJ, Carlsen J, Cumming P, Bylund J, Luebbers T, Bartenstein P, Steiner H, Haass C, Baumann K, Rominger A (2015) Amyloid-PET predicts inhibition of de novo plaque formation upon chronic γ-secretase modulator treatment. *Mol Psychiatry* **20**, 1179-1187.

[39] Villemagne VL, Chételat G (2016) Neuroimaging biomarkers in Alzheimer's disease and other dementias. *Ageing Res Rev* **30**, 4-16.

[40] Lebedeva A, Westman E, Lebedev AV, Li X, Winblad B, Simmons A, Wahlund LO, Aarsland D; Alzheimer's Disease Neuroimaging Initiative (2014) Structural brain changes associated with depressive symptoms in the elderly with Alzheimer's disease. *J Neurol Neurosurg Psychiatry* **85**, 930-935.

[41] Lee GJ, Lu PH, Hua X, Lee S, Wu S, Nguyen K, Teng E, Leow AD, Jack CR Jr, Toga AW, Weiner MW, Bartzokis G, Thompson PM, Alzheimer's Disease Neuroimaging Initiative (2012) Depressive symptoms in mild cognitive impairment predict greater atrophy in Alzheimer's disease-related regions. *Biol Psychiatry* **71**, 814-821.

[42] Du MY, Wu QZ, Yue Q, Li J, Liao Y, Kuang WH, Huang XQ, Chan RC, Mechelli A, Gong QY (2012) Voxelwise meta-analysis of gray matter reduction in major depressive disorder. *Prog Neuropsychopharmacol Biol Psychiatry* **36**, 11-16.

[43] Wang WY, Yu JT, Liu Y, Yin RH, Wang HF, Wang J, Tan L, Radua J, Tan L (2015) Voxel-based meta-analysis of grey matter changes in Alzheimer's disease. *Transl Neurodegener* **4**, 6.

[44] Price JL, Drevets WC (2010) Neurocircuitry of mood disorders. *Neuropsychopharmacology* **35**, 192-216.

[45] Meyer JH, Wilson AA, Ginovart N, Goulding V, Hussey D, Hood K, Houle S (2001) Occupancy of serotonin transporters by paroxetine and citalopram during treatment of depression: A [(11)C]DASB PET imaging study. *Am J Psychiatry* **158**, 1843-1849.

[46] Nakajima S, Uchida H, Suzuki T, Watanabe K, Hirano J, Yagihashi T, Takeuchi H, Abe T, Kashima H, Mimura M (2011) Is switching antidepressants following early nonresponse more beneficial in acute-phase treatment of depression?: A randomized open-label trial. *Prog Neuropsychopharmacol Biol Psychiatry* **35**, 1983-1989.

[47] Holland D, McEvoy LK, Dale AM; Alzheimer's Disease Neuroimaging Initiative (2012) Unbiased comparison of sample size estimates from longitudinal structural measures in ADNI. *Hum Brain Mapp* **33**, 2586-2602.

7. Abkürzungsverzeichnis

Aβ = β-Amyloid

AD = Alzheimer-Krankheit

ADAS-Cog/ ADAS = Alzheimer's Disease Assessment Scale Cognition

ADNI = Alzheimer's Disease Neuroimaging Initiative

APP = Amyloid-Vorläufer-Protein (Amyloid Precursor Protein)

^{11}C-PiB = ^{11}C-Pittsburgh Compound B

^{18}F-AV45 = ^{18}F Florbetapir (Amyloid-Tracer)

FWE = Familywise Error

HC = gesunde Kontrollpersonen (Healthy Control)

HWZ = Halbwertszeit

MCI =Leichte Kognitive Beeinträchtigung (Mild Cognitive Impairment)

MMSE = Mini-Mental-Status-Test (Mini Mental State Examination)

MNI = Montreal Neurological Institute

MRT = Magnet-Resonanz-Tomographie

NPI-Q-Scores = Neuropsychiatric Inventory–Questionnaire-Scores

PET = Positronen-Emissions-Tomographie

SSRI = Selektive Serotonin-Wiederaufnahme-Inhibitoren (Selective Serotonine-Reuptake-Inhibitor)

SUVR = Standard-Uptake-Value-Ratio

VOI = Volume-Of-Interest

8. Literaturverzeichnis

Barthel, H., H. J. Gertz, S. Dresel, O. Peters, P. Bartenstein, K. Buerger, F. Hiemeyer, S. M. Wittemer-Rump, J. Seibyl, C. Reininger, O. Sabri and G. Florbetaben Study (2011). "Cerebral amyloid-beta PET with florbetaben (18F) in patients with Alzheimer's disease and healthy controls: a multicentre phase 2 diagnostic study." Lancet Neurol **10**(5): 424-435.

Braak, H. and E. Braak (1995). "Staging of Alzheimer's disease-related neurofibrillary changes." Neurobiol Aging **16**(3): 271-278; discussion 278-284.

Brendel, M., M. Hogenauer, A. Delker, J. Sauerbeck, P. Bartenstein, J. Seibyl, A. Rominger and I. Alzheimer's Disease Neuroimaging (2015). "Improved longitudinal [(18)F]-AV45 amyloid PET by white matter reference and VOI-based partial volume effect correction." Neuroimage **108**: 450-459.

Brendel, M., J. Sauerbeck, S. Greven, S. Kotz, F. Scheiwein, J. Blautzik, A. Delker, O. Pogarell, K. Ishii, P. Bartenstein, A. Rominger and I. Alzheimer's Disease Neuroimaging (2018). "Serotonin Selective Reuptake Inhibitor Treatment Improves Cognition and Grey Matter Atrophy but not Amyloid Burden During Two-Year Follow-Up in Mild Cognitive Impairment and Alzheimer's Disease Patients with Depressive Symptoms." J Alzheimers Dis **65**(3): 793-806.

Brendel, M., J. Schnabel, S. Schonecker, L. Wagner, E. Brendel, J. Meyer-Wilmes, M. Unterrainer, A. Schildan, M. Patt, C. Prix, N. Ackl, C. Catak, O. Pogarell, J. Levin, A. Danek, K. Buerger, P. Bartenstein, H. Barthel, O. Sabri and A. Rominger (2017). "Additive value of amyloid-PET in routine cases of clinical dementia work-up after FDG-PET." Eur J Nucl Med Mol Imaging **44**(13): 2239-2248.

Buckner, R. L., A. Z. Snyder, B. J. Shannon, G. LaRossa, R. Sachs, A. F. Fotenos, Y. I. Sheline, W. E. Klunk, C. A. Mathis, J. C. Morris and M. A. Mintun (2005). "Molecular, structural, and functional characterization of Alzheimer's disease: evidence for a relationship between default activity, amyloid, and memory." J Neurosci **25**(34): 7709-7717.

Budd Haeberlein, S., P. S. Aisen, F. Barkhof, S. Chalkias, T. Chen, S. Cohen, G. Dent, O. Hansson, K. Harrison, C. von Hehn, T. Iwatsubo, C. Mallinckrodt, C. J. Mummery, K. K. Muralidharan, I. Nestorov, L. Nisenbaum, R. Rajagovindan, L. Skordos, Y. Tian, C. H. van Dyck, B. Vellas, S. Wu, Y. Zhu and A. Sandrock (2022). "Two Randomized Phase 3 Studies of Aducanumab in Early Alzheimer's Disease." J Prev Alzheimers Dis **9**(2): 197-210.

Chiaravalloti, A., R. Danieli, A. Lacanfora, B. Palumbo, C. Caltagirone and O. Schillaci (2017). "Usefulness of 18F Florbetaben in Diagnosis of Alzheimer's Disease and Other Types of Dementia." Curr Alzheimer Res **14**(2): 154-160.

Cirrito, J. R., B. M. Disabato, J. L. Restivo, D. K. Verges, W. D. Goebel, A. Sathyan, D. Hayreh, G. D'Angelo, T. Benzinger, H. Yoon, J. Kim, J. C. Morris, M. A. Mintun and Y. I. Sheline (2011). "Serotonin signaling is associated with lower amyloid-beta levels and plaques in transgenic mice and humans." Proc Natl Acad Sci U S A **108**(36): 14968-14973.

Creavin, S. T., S. Wisniewski, A. H. Noel-Storr, C. M. Trevelyan, T. Hampton, D. Rayment, V. M. Thom, K. J. Nash, H. Elhamoui, R. Milligan, A. S. Patel, D. V. Tsivos, T. Wing, E. Phillips, S. M. Kellman, H. L. Shackleton, G. F. Singleton, B. E. Neale, M. E. Watton and S. Cullum (2016). "Mini-Mental State Examination (MMSE) for the detection of dementia in clinically unevaluated people aged 65 and over in community and primary care populations." Cochrane Database Syst Rev(1): CD011145.

Curtis, C., J. E. Gamez, U. Singh, C. H. Sadowsky, T. Villena, M. N. Sabbagh, T. G. Beach, R. Duara, A. S. Fleisher, K. A. Frey, Z. Walker, A. Hunjan, C. Holmes, Y. M. Escovar, C. X. Vera, M. E. Agronin, J. Ross, A. Bozoki, M. Akinola, J. Shi, R. Vandenberghe, M. D. Ikonomovic, P. F. Sherwin, I. D. Grachev, G. Farrar, A. P. Smith, C. J. Buckley, R. McLain and S. Salloway (2015). "Phase 3 trial of flutemetamol labeled with radioactive fluorine 18 imaging and neuritic plaque density." JAMA Neurol **72**(3): 287-294.

Engler, H., A. Forsberg, O. Almkvist, G. Blomquist, E. Larsson, I. Savitcheva, A. Wall, A. Ringheim, B. Langstrom and A. Nordberg (2006). "Two-year follow-up of amyloid deposition in patients with Alzheimer's disease." Brain **129**(Pt 11): 2856-2866.

Epperly, T., M. A. Dunay and J. L. Boice (2017). "Alzheimer Disease: Pharmacologic and Nonpharmacologic Therapies for Cognitive and Functional Symptoms." Am Fam Physician **95**(12): 771-778.

Fukumoto, H., A. Asami-Odaka, N. Suzuki, H. Shimada, Y. Ihara and T. Iwatsubo (1996). "Amyloid beta protein deposition in normal aging has the same characteristics as that in Alzheimer's disease. Predominance of A beta 42(43) and association of A beta 40 with cored plaques." Am J Pathol **148**(1): 259-265.

Grontvedt, G. R., T. N. Schroder, S. B. Sando, L. White, G. Brathen and C. F. Doeller (2018). "Alzheimer's disease." Curr Biol **28**(11): R645-R649.

Guo, T., M. Brendel, T. Grimmer, A. Rominger, I. Yakushev and I. Alzheimer's Disease Neuroimaging (2017). "Predicting Regional Pattern of Longitudinal beta-Amyloid Accumulation by Baseline PET." J Nucl Med **58**(4): 639-645.

Heurling, K., A. Leuzy, E. R. Zimmer, M. Lubberink and A. Nordberg (2016). "Imaging beta-amyloid using [(18)F]flutemetamol positron emission tomography: from dosimetry to clinical diagnosis." Eur J Nucl Med Mol Imaging **43**(2): 362-373.

Ikonomovic, M. D., W. E. Klunk, E. E. Abrahamson, C. A. Mathis, J. C. Price, N. D. Tsopelas, B. J. Lopresti, S. Ziolko, W. Bi, W. R. Paljug, M. L. Debnath, C. E. Hope, B. A. Isanski, R. L. Hamilton and S. T. DeKosky (2008). "Post-mortem correlates of in vivo PiB-PET amyloid imaging in a typical case of Alzheimer's disease." Brain **131**(Pt 6): 1630-1645.

Ishibashi, K., K. Ishiwata, J. Toyohara, S. Murayama and K. Ishii (2014). "Regional analysis of striatal and cortical amyloid deposition in patients with Alzheimer's disease." Eur J Neurosci **40**(4): 2701-2706.

Jack, C. R., Jr., D. A. Bennett, K. Blennow, M. C. Carrillo, B. Dunn, S. B. Haeberlein, D. M. Holtzman, W. Jagust, F. Jessen, J. Karlawish, E. Liu, J. L. Molinuevo, T. Montine, C. Phelps, K. P. Rankin, C. C. Rowe, P. Scheltens, E. Siemers, H. M. Snyder, R. Sperling and Contributors (2018). "NIA-AA Research Framework: Toward a biological definition of Alzheimer's disease." Alzheimers Dement **14**(4): 535-562.

Jack, C. R., Jr. and D. M. Holtzman (2013). "Biomarker modeling of Alzheimer's disease." Neuron **80**(6): 1347-1358.

Johnson, K. A., S. Minoshima, N. I. Bohnen, K. J. Donohoe, N. L. Foster, P. Herscovitch, J. H. Karlawish, C. C. Rowe, M. C. Carrillo, D. M. Hartley, S. Hedrick, V. Pappas and W. H. Thies (2013). "Appropriate use criteria for amyloid PET: a report of the Amyloid Imaging Task Force, the Society of Nuclear Medicine and Molecular Imaging, and the Alzheimer's Association." J Nucl Med **54**(3): 476-490.

Joshi, A. D., M. J. Pontecorvo, C. M. Clark, A. P. Carpenter, D. L. Jennings, C. H. Sadowsky, L. P. Adler, K. D. Kovnat, J. P. Seibyl, A. Arora, K. Saha, J. D. Burns, M. J. Lowrey, M. A.

Mintun, D. M. Skovronsky and F. S. I. Florbetapir (2012). "Performance characteristics of amyloid PET with florbetapir F 18 in patients with alzheimer's disease and cognitively normal subjects." J Nucl Med **53**(3): 378-384.

Klunk, W. E., H. Engler, A. Nordberg, Y. Wang, G. Blomqvist, D. P. Holt, M. Bergstrom, I. Savitcheva, G. F. Huang, S. Estrada, B. Ausen, M. L. Debnath, J. Barletta, J. C. Price, J. Sandell, B. J. Lopresti, A. Wall, P. Koivisto, G. Antoni, C. A. Mathis and B. Langstrom (2004). "Imaging brain amyloid in Alzheimer's disease with Pittsburgh Compound-B." Ann Neurol **55**(3): 306-319.

Kobylecki, C., T. Langheinrich, R. Hinz, E. R. Vardy, G. Brown, M. E. Martino, C. Haense, A. M. Richardson, A. Gerhard, J. M. Anton-Rodriguez, J. S. Snowden, D. Neary, M. J. Pontecorvo and K. Herholz (2015). "18F-florbetapir PET in patients with frontotemporal dementia and Alzheimer disease." J Nucl Med **56**(3): 386-391.

Koivunen, J., N. Scheinin, J. R. Virta, S. Aalto, T. Vahlberg, K. Nagren, S. Helin, R. Parkkola, M. Viitanen and J. O. Rinne (2011). "Amyloid PET imaging in patients with mild cognitive impairment: a 2-year follow-up study." Neurology **76**(12): 1085-1090.

Kozin, S. A., E. P. Barykin, V. A. Mitkevich and A. A. Makarov (2018). "Anti-amyloid Therapy of Alzheimer's Disease: Current State and Prospects." Biochemistry (Mosc) **83**(9): 1057-1067.

Kueper, J. K., M. Speechley and M. Montero-Odasso (2018). "The Alzheimer's Disease Assessment Scale-Cognitive Subscale (ADAS-Cog): Modifications and Responsiveness in Pre-Dementia Populations. A Narrative Review." J Alzheimers Dis **63**(2): 423-444.

Leuzy, A., I. Savitcheva, K. Chiotis, J. Lilja, P. Andersen, N. Bogdanovic, V. Jelic and A. Nordberg (2019). "Clinical impact of [(18)F]flutemetamol PET among memory clinic patients with an unclear diagnosis." Eur J Nucl Med Mol Imaging **46**(6): 1276-1286.

McKhann, G. M., D. S. Knopman, H. Chertkow, B. T. Hyman, C. R. Jack, Jr., C. H. Kawas, W. E. Klunk, W. J. Koroshetz, J. J. Manly, R. Mayeux, R. C. Mohs, J. C. Morris, M. N. Rossor, P. Scheltens, M. C. Carrillo, B. Thies, S. Weintraub and C. H. Phelps (2011). "The diagnosis of dementia due to Alzheimer's disease: recommendations from the National Institute on Aging-Alzheimer's Association workgroups on diagnostic guidelines for Alzheimer's disease." Alzheimers Dement **7**(3): 263-269.

Mukhopadhyay, S. and D. Banerjee (2021). "A Primer on the Evolution of Aducanumab: The First Antibody Approved for Treatment of Alzheimer's Disease." J Alzheimers Dis **83**(4): 1537-1552.

Nordberg, A., J. O. Rinne, A. Kadir and B. Langstrom (2010). "The use of PET in Alzheimer disease." Nat Rev Neurol **6**(2): 78-87.

Patterson, C. (2018). "World Alzheimer Report 2018; The state of the art of dementia research: New frontiers." Alzheimer’s Disease International.

Rabinovici, G. D., A. J. Furst, J. P. O'Neil, C. A. Racine, E. C. Mormino, S. L. Baker, S. Chetty, P. Patel, T. A. Pagliaro, W. E. Klunk, C. A. Mathis, H. J. Rosen, B. L. Miller and W. J. Jagust (2007). "11C-PIB PET imaging in Alzheimer disease and frontotemporal lobar degeneration." Neurology **68**(15): 1205-1212.

Reynolds, G. P., S. L. Mason, A. Meldrum, S. De Keczer, H. Parnes, R. M. Eglen and E. H. Wong (1995). "5-Hydroxytryptamine (5-HT)4 receptors in post mortem human brain tissue: distribution, pharmacology and effects of neurodegenerative diseases." Br J Pharmacol **114**(5): 993-998.

Rowe, C. C., U. Ackerman, W. Browne, R. Mulligan, K. L. Pike, G. O'Keefe, H. Tochon-Danguy, G. Chan, S. U. Berlangieri, G. Jones, K. L. Dickinson-Rowe, H. P. Kung, W. Zhang, M. P. Kung, D. Skovronsky, T. Dyrks, G. Holl, S. Krause, M. Friebe, L. Lehman, S. Lindemann, L. M. Dinkelborg, C. L. Masters and V. L. Villemagne (2008). "Imaging of amyloid beta in Alzheimer's disease with 18F-BAY94-9172, a novel PET tracer: proof of mechanism." Lancet Neurol **7**(2): 129-135.

Sauerbeck, J., K. Ishii, C. Hosokawa, H. Kaida, F. T. Scheiwein, K. Hanaoka, A. Rominger, M. Brendel, P. Bartenstein and T. Murakami (2018). "The correlation between striatal and cortical binding ratio of (11)C-PiB-PET in amyloid-uptake-positive patients." Ann Nucl Med **32**(6): 398-403.

Schonecker, S., C. Prix, T. Raiser, N. Ackl, E. Wlasich, G. Stenglein-Krapf, E. Mille, M. Brendel, O. Sabri, M. Patt, H. Barthel, P. Bartenstein, J. Levin, A. Rominger and A. Danek (2017). "[Amyloid positron-emission-tomography with [(18) F]-florbetaben in the diagnostic workup of dementia patients]." Nervenarzt **88**(2): 156-161.

Sevigny, J., P. Chiao, T. Bussiere, P. H. Weinreb, L. Williams, M. Maier, R. Dunstan, S. Salloway, T. Chen, Y. Ling, J. O'Gorman, F. Qian, M. Arastu, M. Li, S. Chollate, M. S. Brennan, O. Quintero-Monzon, R. H. Scannevin, H. M. Arnold, T. Engber, K. Rhodes, J. Ferrero, Y. Hang, A. Mikulskis, J. Grimm, C. Hock, R. M. Nitsch and A. Sandrock (2016). "The antibody aducanumab reduces Abeta plaques in Alzheimer's disease." Nature **537**(7618): 50-56.

Sevigny, J., J. Suhy, P. Chiao, T. Chen, G. Klein, D. Purcell, J. Oh, A. Verma, M. Sampat and J. Barakos (2016). "Amyloid PET Screening for Enrichment of Early-Stage Alzheimer Disease Clinical Trials: Experience in a Phase 1b Clinical Trial." Alzheimer Dis Assoc Disord **30**(1): 1-7.

Sheline, Y. I., T. West, K. Yarasheski, R. Swarm, M. S. Jasielec, J. R. Fisher, W. D. Ficker, P. Yan, C. Xiong, C. Frederiksen, M. V. Grzelak, R. Chott, R. J. Bateman, J. C. Morris, M. A. Mintun, J. M. Lee and J. R. Cirrito (2014). "An antidepressant decreases CSF Abeta production in healthy individuals and in transgenic AD mice." Sci Transl Med **6**(236): 236re234.

Sojkova, J., Y. Zhou, Y. An, M. A. Kraut, L. Ferrucci, D. F. Wong and S. M. Resnick (2011). "Longitudinal patterns of beta-amyloid deposition in nondemented older adults." Arch Neurol **68**(5): 644-649.

Tan, C. C., J. T. Yu, H. F. Wang, M. S. Tan, X. F. Meng, C. Wang, T. Jiang, X. C. Zhu and L. Tan (2014). "Efficacy and safety of donepezil, galantamine, rivastigmine, and memantine for the treatment of Alzheimer's disease: a systematic review and meta-analysis." J Alzheimers Dis **41**(2): 615-631.

Trivino-Ibanez, E. M., R. Sanchez-Vano, P. Sopena-Novales, J. C. Romero-Fabrega, A. Rodriguez-Fernandez, C. Carnero Pardo, M. D. Martinez Lozano and M. Gomez-Rio (2019). "Impact of amyloid-PET in daily clinical management of patients with cognitive impairment fulfilling appropriate use criteria." Medicine (Baltimore) **98**(29): e16509.

van Dyck, C. H. (2018). "Anti-Amyloid-beta Monoclonal Antibodies for Alzheimer's Disease: Pitfalls and Promise." Biol Psychiatry **83**(4): 311-319.

Vellas, B., M. C. Carrillo, C. Sampaio, H. R. Brashear, E. Siemers, H. Hampel, L. S. Schneider, M. Weiner, R. Doody, Z. Khachaturian, J. Cedarbaum, M. Grundman, K. Broich, E. Giacobini, B. Dubois, R. Sperling, G. K. Wilcock, N. Fox, P. Scheltens, J. Touchon, S. Hendrix, S. Andrieu, P. Aisen and E. U. C. T. F. Members (2013). "Designing drug trials for

Alzheimer's disease: what we have learned from the release of the phase III antibody trials: a report from the EU/US/CTAD Task Force." Alzheimers Dement **9**(4): 438-444.

Villain, N., G. Chetelat, B. Grassiot, P. Bourgeat, G. Jones, K. A. Ellis, D. Ames, R. N. Martins, F. Eustache, O. Salvado, C. L. Masters, C. C. Rowe, V. L. Villemagne and A. R. Group (2012). "Regional dynamics of amyloid-beta deposition in healthy elderly, mild cognitive impairment and Alzheimer's disease: a voxelwise PiB-PET longitudinal study." Brain **135**(Pt 7): 2126-2139.

Villemagne, V. L., S. Burnham, P. Bourgeat, B. Brown, K. A. Ellis, O. Salvado, C. Szoeke, S. L. Macaulay, R. Martins, P. Maruff, D. Ames, C. C. Rowe, C. L. Masters, B. Australian Imaging and G. Lifestyle Research (2013). "Amyloid beta deposition, neurodegeneration, and cognitive decline in sporadic Alzheimer's disease: a prospective cohort study." Lancet Neurol **12**(4): 357-367.

Villemagne, V. L., R. S. Mulligan, S. Pejoska, K. Ong, G. Jones, G. O'Keefe, J. G. Chan, K. Young, H. Tochon-Danguy, C. L. Masters and C. C. Rowe (2012). "Comparison of 11C-PiB and 18F-florbetaben for Abeta imaging in ageing and Alzheimer's disease." Eur J Nucl Med Mol Imaging **39**(6): 983-989.

Weiner, M. W., P. S. Aisen, C. R. Jack, Jr., W. J. Jagust, J. Q. Trojanowski, L. Shaw, A. J. Saykin, J. C. Morris, N. Cairns, L. A. Beckett, A. Toga, R. Green, S. Walter, H. Soares, P. Snyder, E. Siemers, W. Potter, P. E. Cole, M. Schmidt and I. Alzheimer's Disease Neuroimaging (2010). "The Alzheimer's disease neuroimaging initiative: progress report and future plans." Alzheimers Dement **6**(3): 202-211 e207.

Weiner, M. W., D. P. Veitch, P. S. Aisen, L. A. Beckett, N. J. Cairns, R. C. Green, D. Harvey, C. R. Jack, Jr., W. Jagust, J. C. Morris, R. C. Petersen, J. Salazar, A. J. Saykin, L. M. Shaw, A. W. Toga, J. Q. Trojanowski and I. Alzheimer's Disease Neuroimaging (2017). "The Alzheimer's Disease Neuroimaging Initiative 3: Continued innovation for clinical trial improvement." Alzheimers Dement **13**(5): 561-571.

Wolz, R., A. J. Schwarz, K. R. Gray, P. Yu, D. L. Hill and I. Alzheimer's Disease Neuroimaging (2016). "Enrichment of clinical trials in MCI due to AD using markers of amyloid and neurodegeneration." Neurology **87**(12): 1235-1241.

Yamin, G. and D. B. Teplow (2017). "Pittsburgh Compound-B (PiB) binds amyloid beta-protein protofibrils." J Neurochem **140**(2): 210-215.

9. Eidesstattliche Versicherung

Ich, Julia Johanna Sauerbeck, erkläre hiermit an Eides statt, dass ich die vorliegende Dissertation mit dem Thema:

„Die Positronen-Emissions-Tomographie zur Beurteilung der zerebralen Amyloid-Verteilung sowie der pharmakologischen Effekte einer Serotonin-Wiederaufnahme-Hemmung“

selbständig verfasst, mich außer der angegebenen keiner weiteren Hilfsmittel bedient und alle Erkenntnisse, die aus dem Schrifttum ganz oder annähernd übernommen sind, als solche kenntlich gemacht und nach ihrer Herkunft unter Bezeichnung der Fundstelle einzeln nachgewiesen habe. Ich erkläre des Weiteren, dass die hier vorgelegte Dissertation nicht in gleicher oder in ähnlicher Form bei einer anderen Stelle zur Erlangung eines akademischen Grades eingereicht wurde.

Hamburg, den 22.12.2022 Julia Johanna Sauerbeck

10. Danksagung

Mein tiefer Dank gilt meinem Doktorvater, Herrn Prof. Dr. med. Axel Rominger, für die Überlassung dieser spannenden und relevanten Thematik und die äußerst engagierte Betreuung. Die Zusammenarbeit war geprägt von einer durchweg angenehmen sowie konstruktiven Arbeitsatmosphäre.

Außerdem möchte ich mich sehr herzlich bei Herrn PD Dr. med. Matthias Brendel bedanken, der durch seine exzellente Einarbeitung, umfangreiche Expertise und mit großer Motivation wesentlich zum Gelingen dieser Arbeit beigetragen hat.

Ich möchte mich zudem bei der gesamten Arbeitsgruppe sowie meinen Mitdoktoranden bedanken für die kollegiale und kurzweilige Zusammenarbeit.

Mein besonderer Dank gilt darüber hinaus Herrn Prof. Dr. med. Peter Bartenstein für die Ermöglichung der Dissertation und die stets konstruktive Unterstützung.

Weiterhin möchte ich der Arbeitsgruppe um Herrn Prof. Kazunari Ishii des „Neurocognitive Disorders Center" des Kindai University Hospitals in Osaka, Japan, für einen Forschungsaufenthalt danken, der sowohl auf professionell-wissenschaftlicher als auch persönlicher Ebene eine enorme Bereicherung darstellte.

Abschließend danke ich von Herzen meinen Eltern, welche mir das Studium und diese Dissertation ermöglichten und mir mit großer Unterstützung und Zuspruch stets zur Seite stehen, sowie Fritz Breckow, der mir insbesondere auf den letzten Metern eine große emotionale Stütze war und immer an mich glaubt.

11. Publikationsliste

Publikationen als Erstautorin im Rahmen der kumulativen Promotion

Sauerbeck J, Ishii K, Hosokawa C, Kaida H, Scheiwein FT, Hanaoka K, Rominger A, Brendel M, Bartenstein P, Murakami T. **The correlation between striatal and cortical binding ratio of 11C-PiB-PET in amyloid-uptake-positive patients.** Ann Nucl Med. 2018

Brendel M*, **Sauerbeck J***, Greven S, Kotz S, Scheiwein F, Blautzik J, Delker A, Pogarell O, Ishii K, Bartenstein P, Rominger A; Alzheimer's Disease Neuroimaging Initiative. **Serotonin Selective Reuptake Inhibitor Treatment Improves Cognition and Grey Matter Atrophy but not Amyloid Burden During Two-Year Follow-Up in Mild Cognitive Impairment and Alzheimer's Disease Patients with Depressive Symptoms.** J Alzheimers Dis. 2018

Weitere Publikationen als Erstautorin

Palleis C*, **Sauerbeck J***, Beyer L, Harris S, Schmitt J, Morenas-Rodriguez E, Finze A, Nitschmann A, Ruch-Rubinstein F, Eckenweber F, Biechele G, Blume T, Shi Y, Weidinger E, Prix C, Bötzel K, Danek A, Rauchmann BS, Stöcklein S, Lindner S, Unterrainer M, Albert NL, Wetzel C, Rupprecht R, Rominger A, Bartenstein P, Herms J, Perneczky R, Haass C, Levin J, Höglinger GU, Brendel M. **In Vivo Assessment of Neuroinflammation in 4-Repeat Tauopathies**. Mov Disord. 2021

Sauerbeck J, Adam G, Meyer M. **Spectral CT in Oncology**. Rofo. 2022

*geteilte Erstautorenschaft

Publikationen als Koautorin

Schmitt J, Palleis C, **Sauerbeck J**, Unterrainer M, Harris S, Prix C, Weidinger E, Katzdobler S, Wagemann O, Danek A, Beyer L, Rauchmann BS, Rominger A, Simons M, Bartenstein P, Perneczky R, Haass C, Levin J, Höglinger GU, Brendel M; German Imaging Initiative for Tauopathies (GII4T). **Dual-Phase β-Amyloid PET Captures Neuronal Injury and Amyloidosis in Corticobasal Syndrome**. Front Aging Neurosci. 2021

Kreuzer A, **Sauerbeck J**, Scheifele M, Stockbauer A, Schönecker S, Prix C, Wlasich E, Loosli SV, M Kazmierczak P, Unterrainer M, Catak C, Janowitz D, Pogarell O, Palleis C, Perneczky R, Albert NL, Bartenstein P, Danek A, Buerger K, Levin J, Zwergal A, Rominger A, Brendel M, Beyer L. **Detection Gap of Right-Asymmetric Neuronal Degeneration by CERAD Test Battery in Alzheimer's Disease**. Front Aging Neurosci. 2021

Beyer L, Meyer-Wilmes J, Schönecker S, Schnabel J, **Sauerbeck J**, Scheifele M, Prix C, Unterrainer M, Catak C, Pogarell O, Palleis C, Perneczky R, Danek A, Buerger K, Bartenstein P, Levin J, Rominger A, Ewers M, Brendel M. **Cognitive reserve hypothesis in frontotemporal dementia: A FDG-PET study**. Neuroimage Clin. 2021

Beyer L, Nitschmann A, Barthel H, van Eimeren T, Unterrainer M, **Sauerbeck J**, Marek K, Song M, Palleis C, Respondek G, Hammes J, Barbe MT, Onur Ö, Jessen F, Saur D, Schroeter ML, Rumpf JJ, Rullmann M, Schildan A, Patt M, Neumaier B, Barret O, Madonia J, Russell DS, Stephens AW, Roeber S, Herms J, Bötzel K, Levin J, Classen J, Höglinger GU, Bartenstein P, Villemagne V, Drzezga A, Seibyl J, Sabri O, Brendel

M. **Early-phase [18F]PI-2620 tau-PET imaging as a surrogate marker of neuronal injury**. Eur J Nucl Med Mol Imaging. 2020

Sacher C, Blume T, Beyer L, Biechele G, **Sauerbeck J**, Eckenweber F, Deussing M, Focke C, Parhizkar S, Lindner S, Gildehaus FJ, von Ungern-Sternberg B, Baumann K, Tahirovic S, Kleinberger G, Willem M, Haass C, Bartenstein P, Cumming P, Rominger A, Herms J, Brendel M. **Asymmetry of Fibrillar Plaque Burden in Amyloid Mouse Models**. J Nucl Med. 2020

Brendel M, Barthel H, van Eimeren T, Marek K, Beyer L, Song M, Palleis C, Gehmeyr M, Fietzek U, Respondek G, **Sauerbeck J**, Nitschmann A, Zach C, Hammes J, Barbe MT, Onur O, Jessen F, Saur D, Schroeter ML, Rumpf JJ, Rullmann M, Schildan A, Patt M, Neumaier B, Barret O, Madonia J, Russell DS, Stephens A, Roeber S, Herms J, Bötzel K, Classen J, Bartenstein P, Villemagne V, Levin J, Höglinger GU, Drzezga A, Seibyl J, Sabri O. **Assessment of 18F-PI-2620 as a Biomarker in Progressive Supranuclear Palsy**. JAMA Neurol. 2020

Ishii K, Yamada T, Hanaoka K, Kaida H, Miyazaki K, Ueda M, Hanada K, Saigoh K, **Sauerbeck J**, Rominger A, Bartenstein P, Kimura Y. **Regional gray matter-dedicated SUVR with 3D-MRI detects positive amyloid deposits in equivocal amyloid PET images**. Ann Nucl Med. 2020

Beyer L, Brendel M, Scheiwein F, **Sauerbeck J**, Hosakawa C, Alberts I, Shi K, Bartenstein P, Ishii K, Seibyl J, Cumming P, Rominger A; Alzheimer's Disease Neuroimaging Initiative. **Improved Risk Stratification for Progression from Mild Cognitive Impairment to Alzheimer's Disease with a Multi-Analytical Evaluation of Amyloid-β Positron Emission Tomography**. J Alzheimers Dis. 2020

Schönecker S, Brendel M, Palleis C, Beyer L, Höglinger GU, Schuh E, Rauchmann BS, **Sauerbeck J**, Rohrer G, Sonnenfeld S, Furukawa K, Ishiki A, Okamura N, Bartenstein P, Dieterich M, Bötzel K, Danek A, Rominger A, Levin J. **PET Imaging of Astrogliosis and Tau Facilitates Diagnosis of Parkinsonian Syndromes.** Front Aging Neurosci. 2019

Brendel M, Schönecker S, Höglinger G, Lindner S, Havla J, Blautzik J, **Sauerbeck J**, Rohrer G, Zach C, Vettermann F, Lang AE, Golbe L, Nübling G, Bartenstein P, Furukawa K, Ishiki A, Bötzel K, Danek A, Okamura N, Levin J, Rominger A. **[18F]-THK5351 PET Correlates with Topology and Symptom Severity in Progressive Supranuclear Palsy**. Front Aging Neurosci. 2018

Blautzik J, Kotz S, Brendel M, **Sauerbeck J**, Vettermann F, Winter Y, Bartenstein P, Ishii K, Rominger A. **Relationship Between Body Mass Index, ApoE4 Status, and PET-Based Amyloid and Neurodegeneration Markers in Amyloid-Positive Subjects with Normal Cognition or Mild Cognitive Impairment.** J Alzheimers Dis. 2017

Blautzik J, Brendel M, **Sauerbeck J**, Kotz S, Scheiwein F, Bartenstein P, Seibyl J, Rominger A. **Reference region selection and the association between the rate of amyloid accumulation over time and the baseline amyloid burden.** European Journal of Nuclear Medicine and Molecular Imaging. 2017

Brendel M, Högenauer M, Delker A, **Sauerbeck J**, Bartenstein P, Seibyl J, Rominger A. **Improved longitudinal [(18)F]-AV45 amyloid PET by white matter reference and VOI-based partial volume effect correction.** Alzheimer's Disease Neuroimaging Initiative. 2015